

# 1 Tectonic interactions during rift linkage: Insights from analog and 2 numerical experiments

3  
4 Timothy Chris Schmid<sup>1</sup>, Sascha Brune<sup>2,3</sup>, Anne Glerum<sup>2</sup>, and Guido Schreurs<sup>1</sup>

5  
6 <sup>1</sup>Institute of Geological Sciences, University of Bern

7 <sup>2</sup>Helmholtz Centre Potsdam – GFZ German Research Centre for Geosciences, Potsdam, Germany

8 <sup>3</sup>University of Potsdam, Potsdam-Golm, Germany

9  
10 Corresponding author Timothy Schmid: [timothy.schmid@geo.unibe.ch](mailto:timothy.schmid@geo.unibe.ch)

11 Institute of Geological Sciences, University of Bern, Baltzerstrasse 1+3, CH-3012 Bern, Switzerland

12  
13 **Keywords:** Numerical modelling, analog modelling, stress deflection, rift interaction, rift  
14 propagation

## 16 Abstract

17 Continental rifts evolve by linkage and interaction of adjacent individual segments. As rift  
18 segments propagate, they can cause notable re-orientation of the local stress field so that  
19 stress orientations deviate from the regional trend. In return, this stress re-orientation can  
20 feed back on progressive deformation and may ultimately deflect propagating rift segments  
21 in an unexpected way. Here, we employ numerical and analog experiments of continental  
22 rifting to investigate the interaction between stress re-orientation and segment linkage. Both  
23 model types employ crustal-scale two-layer setups where pre-existing linear heterogeneities  
24 are introduced by mechanical weak seeds. We test various seed configurations to investigate  
25 the effect of i) two competing rift segments that propagate unilaterally, ii) linkage of two  
26 opposingly propagating rift segments, and iii) the combination of these configurations on  
27 stress re-orientation and rift linkage. Both the analog and numerical models show counter-

28 intuitive rift deflection of two sub-parallel propagating rift segments competing for linkage  
29 with an opposingly propagating segment. The deflection pattern can be explained by means  
30 of stress analysis in numerical experiments where stress re-orientation occurs locally and  
31 propagates across the model domain as rift segments propagate. Major stress re-orientations  
32 may occur locally, which means that faults and rift segment trends do not necessarily align  
33 perpendicularly to far-field extension directions. Our results show that strain localization and  
34 stress re-orientation are closely linked, mutually influence each other and may be an important  
35 factor for rift deflection among competing rift segments as observed in nature.

36

## 37 1. Introduction

38 Continental rifting involves brittle faulting and the formation of subsiding rift basins. In places  
39 where individual rift segments are in proximity, they may interact and link when segments  
40 propagate and the rift system matures (Morley et al., 1990; Nelson et al., 1992; Rosendahl,  
41 1987). The propagation and linkage of formerly isolated rift segments resembles the  
42 propagation and interaction of extension fractures on a micro-scale (e.g., Childs et al., 1995;  
43 Willemse, 1997; Willemse et al., 1996; Fig. 1a). Indeed, analytical solutions and models have  
44 been used to describe crack growth and to predict its direction (e.g., Macdonald and Fox,  
45 1983; Mills, 1981). Such cracks occur in a variety of materials over a vast order of magnitude  
46 in length scale from micro-scale cracks in glass to km-scale ridge interaction structures in  
47 oceanic crust (Pollard and Aydin, 1984; Fig. 1a).

48

49 Propagation and interaction of individual rift segments occur in continental rift systems at  
50 various styles and scales (Fig. 1b) and have been intensively studied over the years. The East  
51 African Rift System (EARS) constitutes a narrow rift with an Eastern and Western branch that  
52 propagate southward and northward, respectively (EARS; e.g., Ebinger et al., 2000; Morley  
53 et al., 1990; Nelson et al., 1992; Bonini et al., 2005; Bosworth, 1985; Brune et al., 2017; Corti

Deleted: eastern

Deleted: western

Moved (insertion) [1]

Moved (insertion) [2]

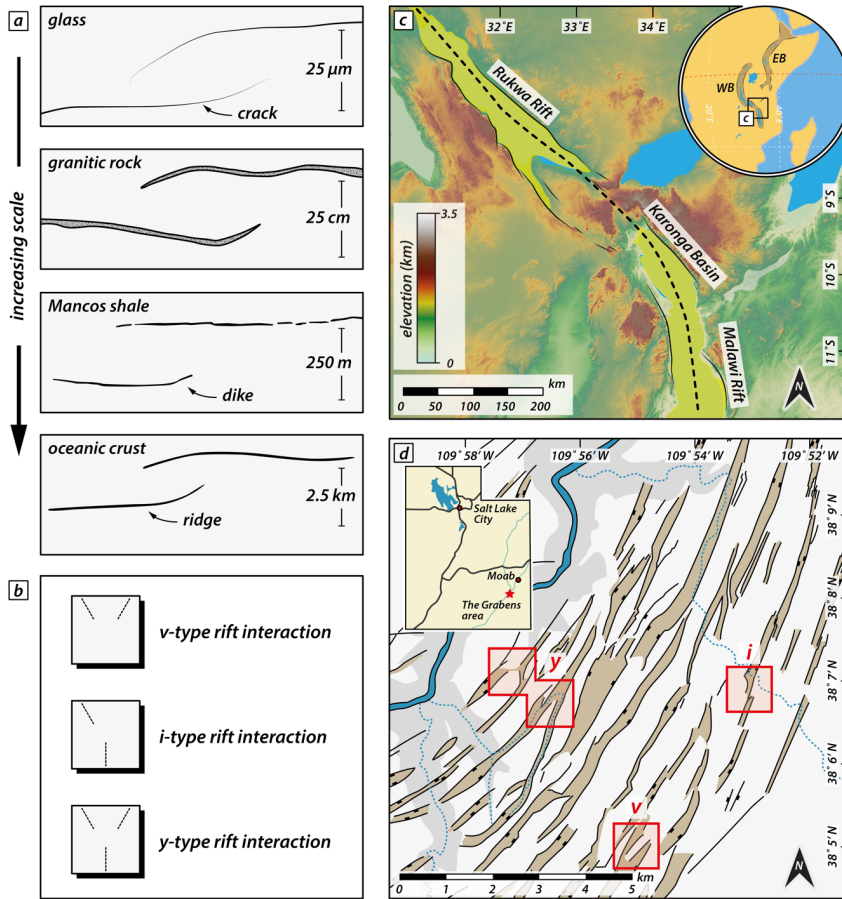
56 et al., 2019; Glerum et al., 2020; Heilman et al., 2019; Koehn et al., 2008; Kolawole et al.,  
 57 2018) comprising different sub-parallel deformed regions (inset Fig. 1c). On smaller scale,  
 58 interaction of segmented grabens has been studied for example in in the Canyonlands National  
 59 Park, Utah, a part of the Basin and Range wide rift (Allken et al., 2013; Trudgill, 2002; Schultz-  
 60 Ela and Walsh, 2002), where various styles of graben interaction are attributed to the  
 61 underlying strata (e.g., salt layer) or pre-existing weaknesses (Fig. 1d).

Moved up [1]: Ebinger et al.,  
 Deleted: 2000;  
 Moved up [2]: 1990; Nelson et al.,  
 Deleted: ; Morley et al.,  
 Deleted: 1992

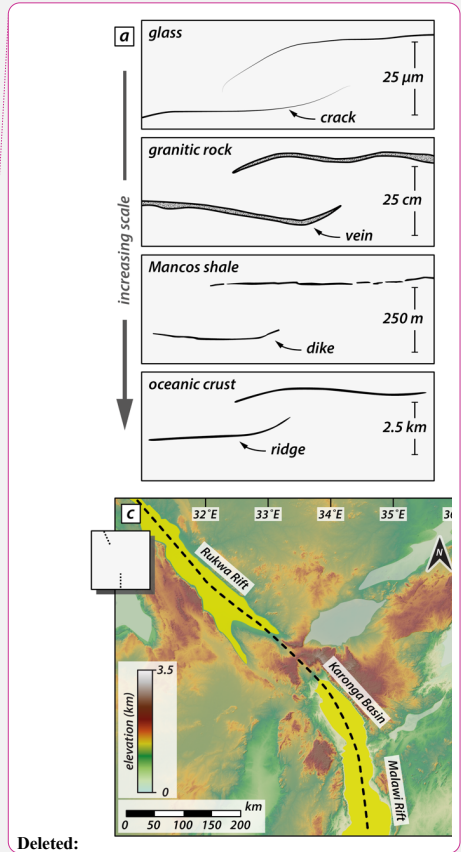
Deleted: , 2002; Trudgill

Deleted: 1b

62



63  
64



Deleted:

73 **Figure 1:** Similar linkage structures occurring at a vast range of spatial scales. a) Propagation and linkage of segments at  
74 different scale from micro cracks in glass to linkage of oceanic ridge segments. Redrawn after Pollard and Aydin, (1984). b)  
75 Rift-interaction types investigated in this study. c) Rukwa Rift and Malawi rift along the Western Branch of the East African  
76 Rift System (EARS; inset). The two basins link obliquely via the Karonga Basin and form an I-type interaction zone. Rift axis  
77 redrawn after Kolawole et al., (2021). WB: Western Branch; EB: Eastern Branch of the EARS. d) Rift-related linked graben  
78 structures in the Canyonlands National Park, USA. Red rectangles mark areas with distinct interaction geometries (v-, i-, and  
79 y-geometries; see [p\)](#) and text for detail). Redrawn after Allken et al., (2013).  
80  
81 Structural inheritance is thought to control nucleation and strain distribution along newly  
82 formed normal faults as weak fabrics can precondition and weaken a heterogenous upper  
83 crust (e.g., Collanega et al., 2018; Heilman et al., 2019; Kolawole et al., 2018; [Morley, 2010;](#)  
84 [Morley, 1999;](#) Kolawole et al., 2021; [Morley, et al., 2004](#)). Pre-existing weak fabrics may appear  
85 as large shear zones (Daly et al., 1989), suture zones along adjacent basement terranes (Corti,  
86 2012; Corti et al., 2007) or upper crustal fabrics. Resulting rift structures may form as initially  
87 isolated segments that propagate along strike, interact and evolve into continuous zones of  
88 deformation with time as they link (Nelson et al., 1992). Rift segments link through previously  
89 un-rifted interaction zones resulting in a characteristic geometry that persists during later rift  
90 stages (Nelson et al., 1992).  
91  
92 Recent strain accommodation in the Rukwa-North Malawi segment of the western branch of  
93 the EARS (Fig. 1c) shows dominant dip-slip faulting parallel to the border faults (Kolawole et  
94 al., 2018; Morley, 2010) driven by the reactivation of pre-existing basement fabrics (Heilman  
95 et al., 2019). There, the concentration of seismicity in the SE and NW of the Rukwa and  
96 Northern Malawi Rift, respectively suggest subsequent propagation and linkage of the rift  
97 segments with a flip in the boundary fault polarity near the interaction zone (Heilman et al.,  
98 2019 and references therein).  
99

Formatted: Line spacing: Double

Moved (insertion) [3]

Deleted: (1984). b

Moved up [3]: (2021).

Deleted: text for detail). Redrawn after Allken et al. (2013).  
c) Rukwa Rift and North Malawi rift in the western branch of the East African Rift System (EARS). The two basins link obliquely via the Karonga Basin and form an interaction zone. Rift axes redrawn after Kolawole et al.

Deleted: d) Turkana Rift on the eastern branch of the EARS. The southward propagating Turkana Rift links with the Suguta Valley that propagates northwards. To the east, the Kino Sogo Fault Belt (KSFB) forms the continuation of the Chew Bahir basin which is part of the Kenyan Rift. Rift axes and faults redrawn after Corti et al. (2019) and Vétel et al. (2005), respectively. Grey insets refer to the geometry of the initial pre-existing weaknesses prior to basin evolution (see text for details...

Formatted: Font: Bold

Deleted: , 2010; Morley, 1999

Moved (insertion) [4]



117 Pre-existing structures as well as fault interaction across multiple scales disturb the regionally  
118 inferred stress orientation (Morley, 2010; Oliva et al., 2022). In return, stress re-orientations  
119 within and adjacent to rift segments influence the style of progressive deformation. Ultimately,  
120 stress re-orientation may even favor pure dip-slip behavior even for extensional faults with an  
121 oblique orientation to the regional extension (e.g., Morley, 2010; Corti et al., 2013; Morley,  
122 2017; Philippon et al., 2015). This interplay between pre-existing structures and local re-  
123 orientation of the regional stress field affects how propagating rift segments interact. Under  
124 favorable conditions, it may even cause deflection of propagating rift segments (Nelson et al.,  
125 1992).

126

127 Rift propagation and segment interaction has been investigated by analog modelling studies  
128 that examined linkage of two segments across a transfer zone (e.g., Zwaan et al., 2016;  
129 Zwaan and Schreurs, 2017; Corti, 2012; Acocella et al., 1999; Bellahsen and Daniel, 2005).  
130 Bellahsen and Daniel (2005) studied the control of existing faults on new fault growth under  
131 multiphase extension. They suggested that pre-existing faults may disturb the local stress field  
132 and impede linkage of newly forming faults, which also occurs in natural examples of  
133 multiphase extension (Duffy et al., 2015). Such stress deflections have been reported and  
134 studied in natural settings such as the North Malay Basin, Thailand, due to the vicinity of pre-  
135 existing faults (Tingay et al., 2006; Tingay et al., 2010). While analog experiments are an  
136 effective tool to simulate mechanical (brittle and ductile) deformation processes occurring in  
137 continental rifts in 3D, accessing information about stresses is challenging. In contrast,  
138 numerical modelling experiments provide direct access to element-wise stress tensors that  
139 can be interpreted in terms of stress regimes and orientations under extension (Brune and  
140 Autin, 2013; Duclaux et al., 2020). Despite the impact of stress distribution on faulting and  
141 rift segment interaction, only recently numerical studies made use of it to gain further insights  
142 into rift evolution and continental break-up (e.g., Glerum et al., 2020; Mondy et al., 2018).

Moved up [4]: may form as initially isolated segments that propagate along strike, interact and evolve into continuous zones of deformation with time as they link (Nelson et al., 1992). Rift segments link through previously un-rifted interaction zones resulting in a characteristic geometry that persists during later rift stages (Nelson et al., 1992).

Deleted: Rifts

Deleted: The interaction zone between the Ethiopian and Kenyan rift of the eastern branch of the EARS comprises different sub-parallel deformed regions (Fig. 1d). The western rift basin corresponds to the N-S trending Turkana Rift that propagated northwestward from the Kenyan Rift via the Suguta Valley (Bonini et al., 2005; Ebinger et al., 2000; Vétel and Le Gall, 2006). The eastern rift corresponds to the Kino Sogo Fault Belt (KSFB) that propagated southward via the Chew Bahir as part of the Ethiopian Rift (Ebinger et al., 2000; Moore Jr and Davidson, 1978; Saria et al., 2014). The two branches form a double-armed system with the KSFB depicting a particular curved faulting style convex to the west along long fault segments with only minor strain accommodation (Vétel et al., 2005). However, the reason for the peculiar shape of the KSFB with its characteristic deformation style remains unclear (Vétel et al., 2005).¶

Deleted: fabrics

Deleted: Olivia

Deleted: 2010,

Deleted: weak fabrics

Deleted: ; Corti, 2012; Zwaan and Schreurs, 2017; Zwaan et al., 2016...

Deleted: .

Deleted: rifting

Deleted: Brune, 2014; Brune and Autin, 2013;

179 However, these studies mostly focus on larger-scale deformation ~~to~~ evaluate stresses over the  
180 entire time span of rifting up to continental break-up.

181

182 Here we use crustal-scale analog and numerical models to investigate rift propagation and  
183 strain localization in early rifting stages when rift segments interact. Both types of models  
184 document enigmatic rift segment deflection when two sub-parallel rift segments propagate  
185 approximately in the same direction and compete for linkage with an opposingly propagating  
186 segment. To understand the reason for rift segment deflection, we analyze the stress  
187 distribution in early rifting stages and its interplay with strain localization that initiates above  
188 pre-existing ~~structures~~. Our experiments show that relatively simple rift segment interactions  
189 can cause locally complex stress patterns that deviate from the regional stress field. Such  
190 stress re-orientations occur in transient stages and can change over time and with progressive  
191 deformation due to subsequent changes in material strengths.

192

Deleted: and

Deleted: weak fabrics

195 **2. Analog model**

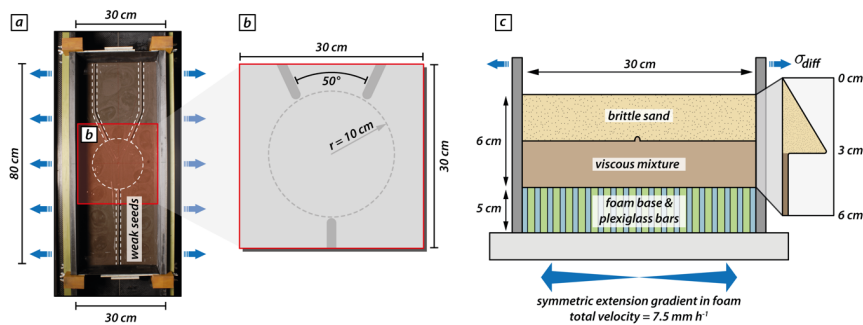
196 The presented analog modelling experiment shows unexpected features such as rift deflection.  
197 It motivates our numerical study, and we use the analog model as a reference for examining  
198 strain and stress distribution in numerical experiments.

199

200 **2.1. Analog model setup**

201 For the analog reference model, we use a simplified two-layer crustal scale setup with a brittle  
202 and a viscous material to simulate upper crustal brittle faulting and lower crustal viscous  
203 deformation, respectively. The base of the model consists of a set of alternating plexiglass  
204 and foam bars which are compressed prior to the model preparation by two mobile sidewalls  
205 (Fig. 2a). During the experiment the computer-controlled sidewalls extend and provide a  
206 symmetric extension gradient as the model base expands and the model vertically thins. For  
207 monitoring the surface deformation evolution, we use a stereoscopic camera setup to take  
208 top view photos and stereo image pairs every 60 s for quantitative deformation analysis by  
209 means of 3D stereo Digital Image Correlation (Adam et al., 2005). The model was scanned  
210 every 20 min in a medical XRCT scanner for gaining insights on internal model evolution.

211



212  
213

214 **Figure 2:** Analog modelling setup. a) Top view of the experimental apparatus with two mobile side walls that extend  
215 orthogonally. The entire model comprises an area of 80 x 30 cm and three viscous seeds are placed on top of the viscous layer  
216 before sieving in the brittle sand layer. The central model part where propagating rift segments interact contains no seeds.

217 b) *Zoom in of the seed configuration into the analyzed model area (i.e., 30 x 30 cm). The two competing seed segments form*  
218 *an intermediate angle of 50°. The model center contains an area with a radius of 10 cm where weak seeds are absent. c)*  
219 *Sketch of the model cross section. The model setup consists of a brittle sand layer representing the upper brittle crust on top*  
220 *of a viscous mixture of PDMS and corundum sand imitating the lower ductile crust.*

Deleted: zoom

221

## 222 2.2. Model geometry, rheological layering, and material properties

223 For simulating upper crustal deformation, we use dry quartz sand with a bulk density of 1560

224 kg m<sup>-3</sup> and an internal friction coefficient of 0.72 (Schmid et al., 2020a). For the lower viscous

Deleted: 2020b

225 model part, we use a quasi-Newtonian PDMS/corundum sand mixture (weight ratio 1:1) with

226 bulk density of 1600 kg m<sup>-3</sup> and a viscosity of  $\sim 1 \times 10^5$  Pa s (Zwaan et al., 2018). Hence, the

Deleted: a

227 brittle-viscous setup has a density gradient that avoids density instabilities and spontaneous

228 upwelling of the viscous layer. The model features viscous rods placed on top of the viscous

229 model layer before sieving in the quartz sand (Fig. 2). These rods act as mechanically weak

Deleted: .

230 seeds and localize faulting in the upper brittle model domain. The used seed configuration

231 includes three individual seed segments. The model includes a y-seed configuration with one

Deleted: One

232 seed segment perpendicular to the extension direction on one side (hereafter called frontal

Deleted: side

233 segment) whereas on the opposing side of the model center two obliquely placed seeds

234 (hereafter called rear segments) form an intermediate angle of 50° (Fig. 2; see also Fig. 1b,d).

Deleted: &

235 The three seed segments hypothetically merge at the model center. However, we exclude

236 weak seeds in an area with a radius  $r = 10$  cm around the model center to allow free

237 interaction of the propagating rift structures (Fig. 2b). The analog model comprises an initial

238 area of 80 cm by 30 cm and has a total thickness of 6 cm (each layer 3 cm) which represents

239 a 30 km thick continental crust. In accordance with the numerical setup, the effectively

240 analyzed model area is restricted to 30 x 30 cm. The mobile sidewalls move with an extension

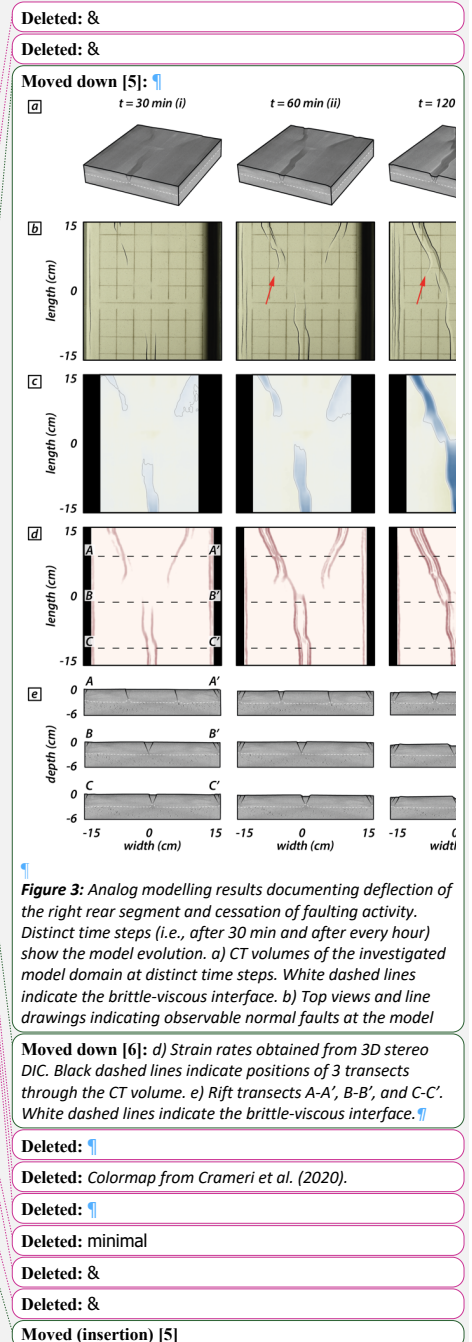
241 velocity of 5 mm h<sup>-1</sup> each (totaling in 10 mm h<sup>-1</sup>), which results in a maximum extension of

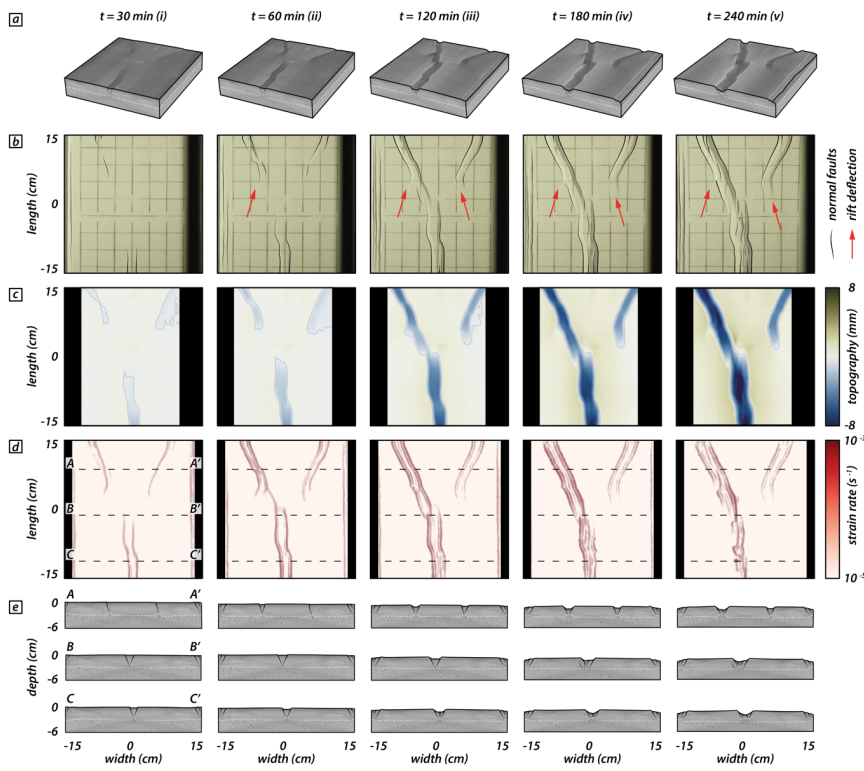
242 40 mm at the final model stage after 4h.

243

### 251 2.3. Analog model results

252 In the analog model three different rift segments initiate above the weak seeds and propagate  
253 toward each other. Thereby, the two rear segments compete for linkage with the frontal  
254 segment. After 30 min (i.e., 5 mm extension; Fig. 3(i)), brittle deformation localizes along two  
255 rift boundary faults forming the frontal rift segment. Rifting in the rear segments localizes first  
256 along right-dipping rift boundary faults and after 60 min (i.e., 10 mm extension; Fig. 3(ii))  
257 both rear segments develop a set of two conjugate rift boundary faults (Fig. 3a,b (ii)).  
258 Interestingly, instead of advancing straight forward, the fault tips deflect and propagate away  
259 from each other (Fig. 3b,d(ii)). This is partially due to the rift propagation over the area where  
260 no seeds are present where rifting perpendicular to the extension direction is favored.  
261 However, after 120 min (i.e., 20 mm extension; Fig. 3 (iii)) rift tips deflect and turn away from  
262 one another. Rift tips deflect from an initially oblique orientation and rotate into an inverted  
263 oblique direction (with respect to the extension direction). The frontal and the rear left rift  
264 segment propagate further and, as they approach one another, form an en-echelon basin that  
265 convergently overlaps with the frontal rift segment (Morley et al., 1990; Fig. 3b,d (iii)). After  
266 180 min (i.e., 30 mm extension; Fig. 3(iv)), intra-rift faults develop in the frontal and left rear  
267 rift segments. Note that strain rate is successively localized in the two fully linked rift segments  
268 whereas the right rear segment experiences minor strain rate values (Fig. 3d (iv)). At the final  
269 model stage (i.e., after 240 min and 40 mm extension; Fig. 3 (v)), the right rear segment  
270 propagated **minimally** with a rift tip turned away from the linked segments (Fig. 3b,d (v)). The  
271 fully linked frontal and left rear segments continuously accommodated displacement resulting  
272 in deeper rift structures compared to the abandoned right rear segment (Fig. 3c,e (v)).





309 **Figure 3:** Analog modelling results documenting deflection of the right rear segment and cessation of faulting activity. Distinct  
 310 time steps (i.e., after 30 min and after every hour) show the model evolution. a) CT volumes of the investigated model domain  
 311 at distinct time steps. White dashed lines indicate the brittle-viscous interface. b) Top views and line drawings indicating  
 312 observable normal faults at the model surface. Red arrows indicate rift tips that deflect and turn away from one another. c)  
 313 Topography from digital elevation models of the model surface. d) Strain rates obtained from 3D stereo DIC. Black dashed  
 314 lines indicate positions of 3 transects through the CT volume. e) Rift transects A-A', B-B', and C-C'. White dashed lines indicate  
 315 the brittle-viscous interface.  
 316  
 317

Moved (insertion) [6]

### 319 3. Numerical modelling

320 We perform a series of numerical models to investigate rift linkage interaction and to analyze  
 321 occurring surface stresses. Similar to the analog experiment, the numerical model consists of  
 322 a two-layer crustal setup with laterally homogenous material layers where boundary-  
 323 orthogonal extension with constant velocity is applied.

### 324 3.1. Numerical model setup

325 We use the open source, finite-element code ASPECT to solve the extended Boussinesq  
326 equations of momentum, mass, and energy in combination with advection equations for each  
327 compositional field (Gassmüller et al., 2018; Glerum et al., 2018; Heister et al., 2017;  
328 Kronbichler et al., 2012; Rose et al., 2017; Glerum et al., 2020). Since the numerical models  
329 are motivated by the analog model, the two setups are designed in a similar way. To this aim,  
330 we employ a numerical setup where the rheologies of upper and lower crust are brittle and  
331 ductile, respectively, and independent of temperature just like in the analog model. However,  
332 the numerical models operate on the true scales of the continental crust over tens of  
333 kilometers and millions of years, while the analog model is a scaled, cm-sized representation  
334 that evolves on hour-scale. Additionally, the numerical setup applies maximum extension  
335 velocities at the side walls and extension velocities at the base that linearly increase from the  
336 center towards the model boundaries. In contrast, maximum extension velocities at the side  
337 walls in the analog model are achieved via compression of a basal foam plexiglass setup (prior  
338 to the model run) that extends homogeneously during the model run.

339  
340 The presented numerical experiments cover a rectangular cuboid domain of 150 km width  
341 and length in the horizontal x- and y-direction, respectively, and 30 km in depth along the  
342 vertical z-axis (Fig. 4a). The entire model domain is divided into 1.53 million hexahedral,  
343 second-order elements. For the upper 15 km of the model, we use a cell resolution of 750 m,  
344 with an additional refinement at the uppermost km which yields near-surface elements with a  
345 resolution of 375 m. The grid resolution for the lower 15 km of the model is 1500 m. At the  
346 left and right model sides, we apply a symmetrically distributed outflow velocity of  $\frac{1}{2} V_x = 5$   
347 mm yr<sup>-1</sup>, resulting in a total extension velocity of 10 mm yr<sup>-1</sup> (Fig. 4a,b). After a total model  
348 time of 4 My, the model has therefore experienced a total extension of 40 km. While  $V_x$  is  
349 prescribed at the left and right model sides,  $V_y$  and  $V_z$  are left free. We compensate material

Deleted: ¶

Deleted: 2020; Glerum et al.,

Deleted: ).

Deleted: set ups

Deleted: set up

Deleted: milion

Deleted: at the surface.

Deleted: &

Deleted: allowed to move freely.

359 loss through the side boundaries by compensational inflow at the model base and the  
360 horizontal  $V_x$  component increases linearly from the model center towards the lateral model  
361 boundaries (Fig. 4b). The front and back lateral boundaries allow for free slip and the top of  
362 the model features a free surface boundary condition (Rose et al., 2017).

363

364 The model includes two rheological layers represented by compositional fields, namely a 15  
365 km thick visco-plastic upper crust with a density of  $2700 \text{ kg m}^{-3}$  and a 15 km thick iso-viscous  
366 lower crust with a density of  $2900 \text{ kg m}^{-3}$  and a constant viscosity of  $1 \cdot 10^{20} \text{ Pa s}$ . For the upper  
367 crust, the viscous viscosity is fixed to  $2 \cdot 10^{28} \text{ Pa s}$ , such that plastic deformation is always  
368 enabled. We introduce initial and dynamic mechanical weaknesses in the upper crust in two  
369 ways. (i) Mechanically weak seeds: At distinct positions near the brittle-ductile interface, the  
370 upper model layer is locally 10% thinned and the lower model layer elevates like the viscous  
371 weak seeds in the analog model setup. These mechanical seeds weaken the upper crustal  
372 strength and localize brittle faulting. Our experiments include three different seed  
373 configurations: v, i, and y (Fig. 4c; see also Fig. 1b-d), where seeds within a central model  
374 area (i.e.,  $r = 100 \text{ km}$ ) are absent. For each configuration, the rear seeds form an intermediate  
375 angle of  $10^\circ$ ,  $30^\circ$ , or  $50^\circ$ . (ii) Friction softening: For each element, an initial plastic strain value  
376 of 0 (resulting in strong material) to 0.1 (weaker) is randomly assigned and reduces the  
377 maximum friction angle of  $26.56^\circ$  by a maximum of 10%. This reflects the structural  
378 heterogeneity of natural settings and allows for more randomized strain patterns in the central  
379 model domain where the mechanical seeds are absent. The initial plastic strain noise is  
380 distributed over the entire model width with an amplitude following a Gaussian curve parallel  
381 to the extension direction that is repeated along the model length (y-direction, Fig. 4d). During  
382 continuous extension, the effective friction angle linearly reduces to 25% of the maximum  
383 friction angle (i.e., to  $6.64^\circ$ ) for plastic strain between 0 and 1 while it remains constant at  
384  $6.64^\circ$  for plastic strains  $> 1$  (Fig. 4e). This corresponds to a reduction of the effective friction

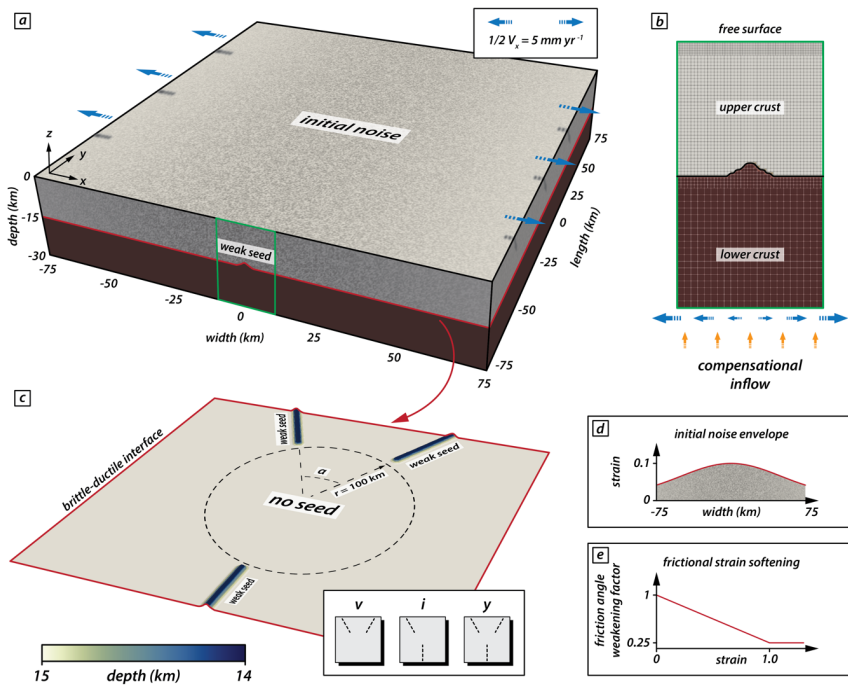
Deleted: ;

Deleted: .



387 coefficient from 0.5 to 0.12. The cohesion of the upper crust remains constant at  $5 \cdot 10^6$  Pa for  
 388 all conducted experiments.

389



390

391

392

393

394

395

396

397

398

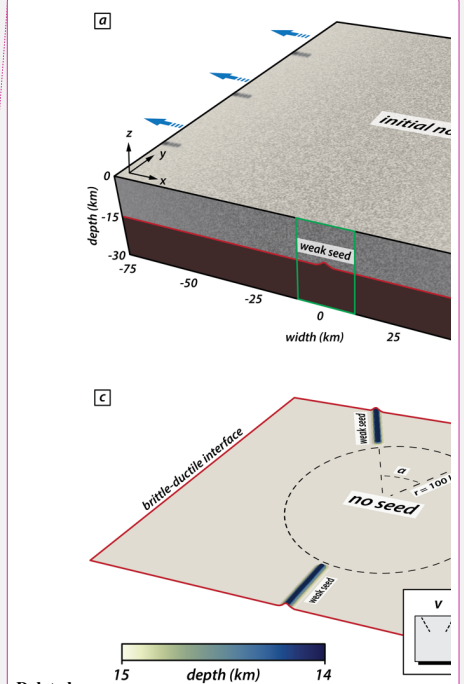
399

400

401

**Figure 4:** Numerical model setup for iso-viscous models. a) The model domain comprises a volume of 150 x 150 x 30 km. Blue arrows indicate the applied boundary-orthogonal extension. The green rectangle indicates the position of the zoom-in in b). The red line indicates the initial depth of the brittle-ductile interface (as defined by the interface between the two rheological layers) indicated in c). b) Initial conditions and mesh refinement (arrows not to scale). c) Position and configuration of the mechanical weak seeds at the brittle-ductile interface. The setup comprises an area with radius  $r = 100$  km where no weak seeds are present. Three different seed configurations refer to  $y$ -,  $i$ -, and  $v$ -models (see text for details). d) Initial amplitude of strain along the  $x$ -axis. The Gaussian distribution is constant along the  $y$ -axis; also see grey shade in a). Note that while the strain amplitude follows a Gaussian distribution, the location of the initial strain is random. e) Linear weakening with strain applied to the friction angle.

Formatted: Line spacing: 1.5 lines



Deleted: Colormap from Cramer et al. (2020).

404 **3.2. Model limitations**

405 Just like the analog model (Sec. 2), our crustal scale two-layer numerical setup does not  
406 comprise a lithospheric mantle layer and no asthenosphere. Further, the iso-viscous setup  
407 does not account for a temperature-dependent viscosity. However, we focus on an early rifting  
408 phase where the influence of the deforming mantle lithosphere can be neglected. The crustal-  
409 scale setup strongly limits the computational effort for calculating deformation in 3D (Allken  
410 et al., 2011, 2012; Katzman et al., 1995; Zwaan et al., 2016) and hence, our simplifications  
411 allow for a higher model resolution; a necessity to depict early stages of rifting and the  
412 coalescence of brittle deformation. Several alternative model runs have been performed  
413 including a temperature- and pressure-dependent viscosity. Those tests reproduced first-order  
414 features (i.e., strain rates, rift geometry and stress distribution) of the presented models in  
415 this study, which further justified the choice of a simplified iso-viscous setup. [Note that we](#)  
416 [apply frictional softening as a function of strain within each cell. For simplicity, we do not](#)  
417 [include normalization accounting for cell size \(Lavie et al., 2000\) nor viscoplastic](#)  
418 [regularization techniques \(Duretz et al., 2019; Jacquy and Cacace, 2020\).](#) Moreover, our  
419 model does not include the influence of melting or magma intrusions nor sedimentation and  
420 erosion.

421

422 **3.3. Post-processing**

423 Numerical models pose the advantage that they grant direct access to stress tensors of each  
424 individual cell. We exploit this opportunity by investigating surface stresses to deduce the  
425 stress regime and the effect of different seed configurations on stress distribution. ASPECT  
426 provides post processors that calculate the magnitude and orientation of the maximum  
427 horizontal stresses and the Regime Stress Ratio (RSR) (Glerum et al., 2020). This stress  
428 regime characterization is calculated according to the scheme of the World Stress Map  
429 (Zoback, 1992). The RSR value maps possible stress regimes to an interval between 0 and 3.

430 For isotropic and homogenous materials, the standard rules of Andersonian faulting are  
431 applied (Anderson, 1905). For RSR values  $< 1$ , faulting occurs in an extensional stress regime  
432 whereas for RSR values  $> 2$  compressive stress regimes generate thrust faults. Strike-slip  
433 faults occur for values  $1 \geq \text{RSR} \geq 2$ . We extract data of maximum horizontal compressive  
434 stress together with the stress regime and investigate them in areas where the strain rate  
435 exceeds a threshold of  $10^{-16} \text{ s}^{-1}$  and deformation occurs. [For visualization, surface stresses](#)  
436 [from an originally unstructured grid are resampled on an equidistant grid.](#)

Deleted: .....

### 438 3.4. General model evolution of the reference model

439 In this section we describe the numerical modelling results focusing particularly on the general  
440 evolution of our reference model with a y-seed configuration and an intermediate seed angle  
441 of  $50^\circ$  (Figure 5). At the early stage (i.e., after 0.5 million years), three distinct rift segments  
442 develop above the initial seed positions bounded by a pair of conjugate rift boundary faults  
443 (Fig. 5a (i)). This early stage is characterized by a symmetric evolution of the two competing  
444 rear segments, which results in a symmetric subsidence inside of the graben structures (Fig.  
445 5b (i)). For each rift segment, faulting activity is localized along the rift boundary faults. In  
446 the central model domain, however, strain rates depict a more distributed deformation pattern  
447 with multiple minor faults (Fig. 5c (i)). Note that the two rear segments propagate and show  
448 curved fault segments that initially deflect and turn away from each other resulting in rift  
449 segments with a curved geometry expressed in the topography (Fig. [5b \(i\)](#)), [similar to the rift](#)  
450 [evolution in the analog model.](#) Once they overlap with the propagating frontal segment, faults  
451 symmetrically curve inwards and towards the frontal segment. The change from localized  
452 strain rates above the seeds to distributed strain rate patterns in the central model domain is  
453 best seen in transects (Fig. 5d (i)).

Deleted: 5b (i)).

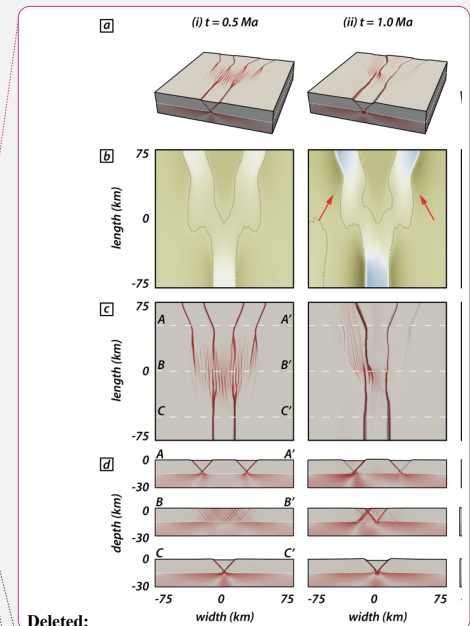
454

457 After the first million years, deformation has prominently localized along the left of the two  
 458 rear segments and along the frontal segment (Fig. 5a,c, (ii)). While deformation in the frontal  
 459 segment is localized along the rift boundary faults, inward migration occurred in the left rear  
 460 segment with developing intra-rift faults and only the left-dipping rift boundary fault active.  
 461 Similarly, the right rear segment shows faulting along the right-dipping rift boundary fault but  
 462 activity along intra-rift faults is lacking. In the central model domain, formerly distributed  
 463 deformation localized between the frontal and left rear rift segment (Fig. 5d (ii)). While strain  
 464 rates indicate a shift from a symmetric to an asymmetric deformation phase, topography is  
 465 still symmetric which implies that the shift is imminent and has not affected the topography  
 466 after the first million years (Fig. 5b (ii)).

467  
 468 After two million years, deformation is entirely localized along the frontal and left rear  
 469 segment. Only the right-dipping rift boundary fault of the frontal segment is active and inward  
 470 migration led to a set of pervasive intra-rift faults (Fig. 5a,c (iii)). The left rear segment depicts  
 471 a similar deformation pattern as in the previous step, but strain mainly accumulates along the  
 472 left-dipping rift boundary fault causing an asymmetric graben geometry (Fig. 5d (iii)). Note  
 473 that, after two million years, fault activity along the right rear segment completely ceased with  
 474 no further strain accumulation visible (Fig. 5a,c,d (iii)). The topography reflects this completed  
 475 switch from a symmetric to an asymmetric deformation stage with enhanced subsidence along  
 476 the frontal and left rear segments and their linkage throughout the central model domain (Fig.  
 477 5b (iii)).

478  
 479 With ongoing extension, deformation subsequently localizes along the axial rift zone that links  
 480 the frontal and left rear segments (Fig. 5a,c,d (iv,v)) and faulting activity along rift boundary  
 481 faults ceases. The linked structure reaches maximum depth inside of the rift after three million  
 482 years. After four million years, however, the basin experiences minor uplift due to increase

Deleted: &



Deleted:

Moved down [7]: ¶

Figure 5: Modelling results of the reference model documenting cessation of faulting activity along the right

Moved down [8]: Distinct time steps show the model evolution. a) Model box showing logarithmic strain rates (red) and plastic strain (black) in the brittle and viscous model domain. White dashed lines indicate the brittle-viscous interface. b) Top views showing the model topography. Red arrows indicate rift tips that deflect and turn away from one another. Black lines refer to the zero

Moved down [9]: c) Top views of the model showing strain rates (red) and corresponding plastic strain (black) at distinct model run times. White dashed lines correspond to the three rift transects A-A', B-B', and C-C' in subfigure d). d) Rift-axis perpendicular transects A-A', B-B', and C-C' parallel to the extension direction. ¶

Deleted: faulting activity along the right rear segment while the left rear, and frontal segments link.

Deleted: elevation height.

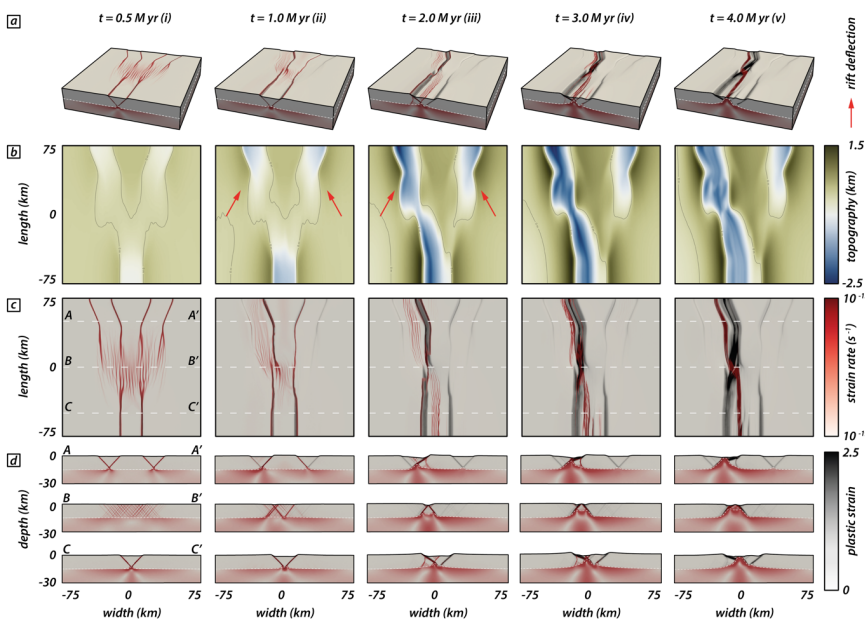
Deleted: &

Deleted: &

Deleted: &

508 upward motion of the underlying viscous material (Fig. 5d (iv,v)). Note that the basin depth  
 509 of the right rear rift segment remains stable after two million years and does not experience  
 510 further subsidence nor uplift.

511



512

513 **Figure 5:** Modelling results of the reference model documenting cessation of fault activity along the right rear segment while  
 514 the left rear and frontal segments link. Distinct time steps show the model evolution. a) Model box showing logarithmic strain  
 515 rates (red) and plastic strain (black) in the brittle and viscous model domain. White dashed lines indicate the brittle-viscous  
 516 interface. b) Top views showing the model topography. Red arrows indicate rift tips that deflect and turn away from one  
 517 another. Black lines refer to the zero-elevation height. c) Top views of the model showing strain rates (red) and corresponding  
 518 plastic strain (black) at distinct model run times. White dashed lines correspond to the three rift transects A-A', B-B', and C-C'  
 519 in subfigure d). d) Rift-axis perpendicular transects A-A', B-B', and C-C' parallel to the extension direction.

521

### 522 3.5. Early localization patterns for v-, i-, and y-seeds

523 To investigate the influence of different seed configurations, we compare v- (Fig. 6a-c), i-  
 524 (Fig. 6d-f), and y-seed (Fig. 6g-i) configurations for different intermediate angles (i.e., 10°,

Moved (insertion) [7]

Moved (insertion) [8]

Moved (insertion) [9]

525 30°, and 50°) at an early stage after 0.5 million years. y- and i-seed configurations provide a  
 526 setup where rift structures opposingly propagate towards the model center where rift linkage  
 527 eventually occurs. In contrast, rift structures in the v-seed configuration propagate  
 528 approximately in the same direction, which has a consequence on the overall strain rate  
 529 distribution.

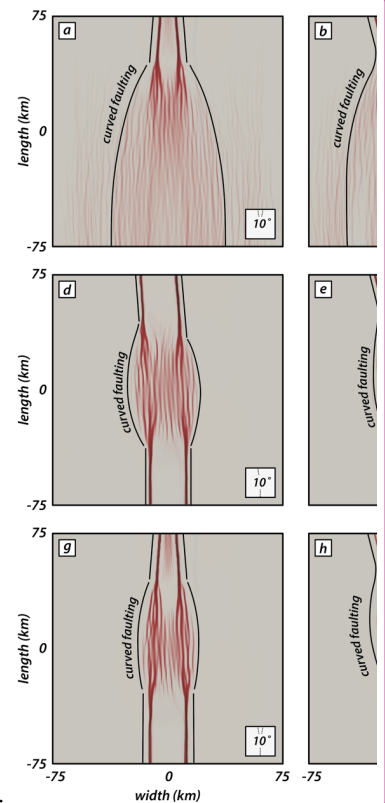
530  
 531 The early stage in v-seed experiments (Fig. 6a-c) is characterized by a zone of localized and  
 532 distributed deformation in the rear and frontal part of the experiments, respectively. The  
 533 transition from localized to distributed deformation occurs where the two competing rift  
 534 segments deflect and rotate away from one another. Note that the fault deflection successively  
 535 decreases towards the left and right model sides, where faults strike perpendicular to the  
 536 extension direction. This is consistent with observations for experiments with a y-seed  
 537 configuration. However, there the two competing rear segments rotate back and eventually  
 538 bend towards the propagating frontal segment (Fig. 6g-i).

540 For experiment with a i-seed configuration (Fig. 6d-f) two opposingly propagating rift branches  
 541 form. Since the right rear segment is absent, both opposingly propagating rift segments link  
 542 in the model center where deformation is distributed onto intra-rift faults. The overall strain  
 543 rate field is localized, and no strain rate deflection occurs.

544  
 545 Models with a y-seed configuration (Fig. 6g-i) depict a strain rate pattern where deformation  
 546 is localized along rift boundary faults at the model margins where seeds are present and a  
 547 distributed en-echelon strain rate pattern in the model center. Note that for the model with  
 548 an intermediate angle of 10° the two competing rear segments are close enough resulting in  
 549 a zone where strain is localized along only one rift boundary fault per rift segment (i.e.,  
 550 outward-dipping faults with respect to the model box) that overlap and form a central graben

Moved down [10]: ¶

**Figure 6:** Types of rift segment linkages depending on the seed configuration at an early phase after 0.5 million years. Model top views show strain rates (logarithmic) and plastic strain in red and black colors, respectively. a-c) v-seed configuration for intermediate angles of 10°, 30°, and 50°. d-f) i-seed configuration for intermediate angles of 10°, 30°, and 50°. g-i) y-seed configuration for intermediate angles of 10°, 30°, and 50° (reference model). Black lines confine deformed areas. Curved faulting occurs wh

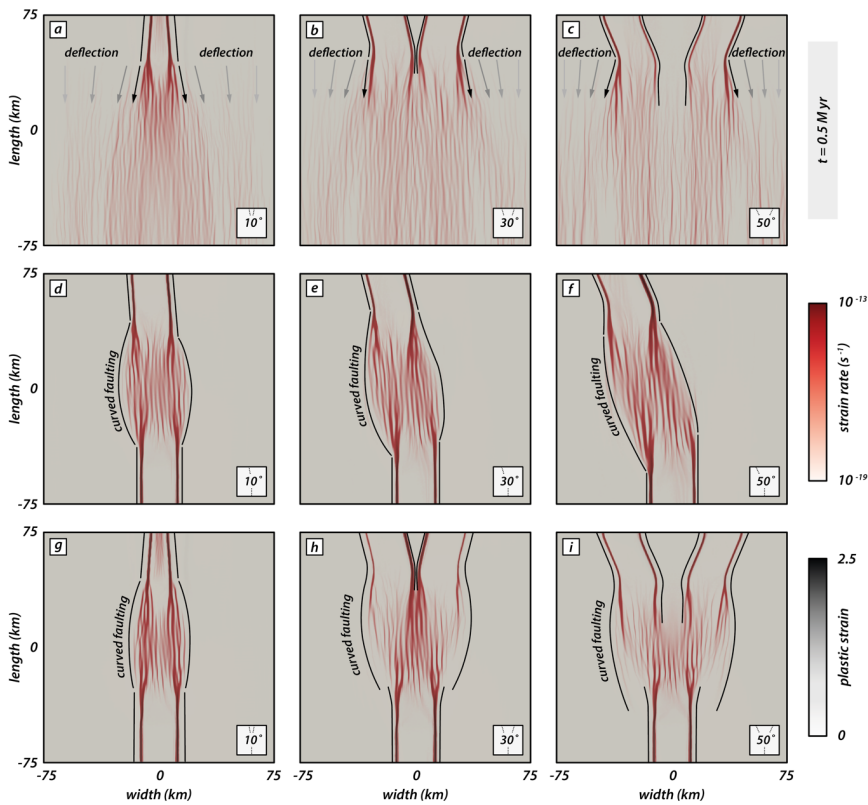


Deleted:

Deleted: Curved faulting occurs where rift segments interact. ¶

564 with minor intra-rift faults. For larger intermediate angles, two individual rift segments  
 565 (bounded by two rift boundary faults) form that propagate towards the model center. While  
 566 the strain rate pattern due to the competing rear segments is identical for experiments with  
 567 a  $\gamma$ - and  $v$ -seed configuration, the additional frontal segment in experiments with a  $\gamma$ -seed  
 568 configuration causes localization of strain rates in a single rift branch bounded by two rift  
 569 boundary faults. This contrasts with the  $v$ -seed configuration where strain rates in the frontal  
 570 model domain occur distributed over the entire model domain (Fig. 6a-c).

571



572  
573

Moved (insertion) [10]

574 **Figure 6:** Types of rift segment linkages depending on the seed configuration at an early phase after 0.5 million years. Model  
 575 top views show strain rates (logarithmic) and plastic strain in red and black colors, respectively. a-c)  $v$ -seed configuration for

576 *intermediate angles of 10°, 30°, and 50°. d-f) i-seed configuration for intermediate angles of 10°, 30°, and 50°. g-i) y-seed*  
577 *configuration for intermediate angles of 10°, 30°, and 50° (reference model). Black lines confine deformed areas. For models*  
578 *with a v-seed configuration (a-c), competing rift segments deflect away from each other resulting in a fan-shaped geometry.*  
579 *Note that fault strike successively re-orientates into an orientation perpendicular to the extension direction towards the left and*  
580 *right model sides. Curved faulting occurs in models with an i- and y-seed configuration (d-i) where rift segments interact.*

581

### 582 **3.6. Final rift geometry and localization patterns for v-, i-, and y-seeds**

583 The final model stage after four million years best illustrates differences in rift geometry  
584 between the models with different seed geometry and an intermediate angle (Fig. 7). Rift  
585 deflection is well visible in v-seed models (Fig. 7 a-c) and most prominent in experiments with  
586 a larger intermediate angle (Fig. 7b,c). Above the seeds, two short individual rift segments  
587 form bounded by a pair of conjugate rift boundary faults. However, as the rifts propagate  
588 towards the model center, strain is mainly accommodated along the boundary faults that dip  
589 towards the model center. Hence, the larger part of the model subsides uniformly and builds  
590 a broad rift zone confined by two large boundary faults. When the two rift segments  
591 propagate, they deflect and turn away from one another resulting in a gradually wider rift.  
592 For intermediate angles of 30° and 50°, both competing rift segments show active faulting  
593 along intra-rift faults in the rear model part, but a zone of continuous faulting activity has  
594 developed along the right side of the rift.

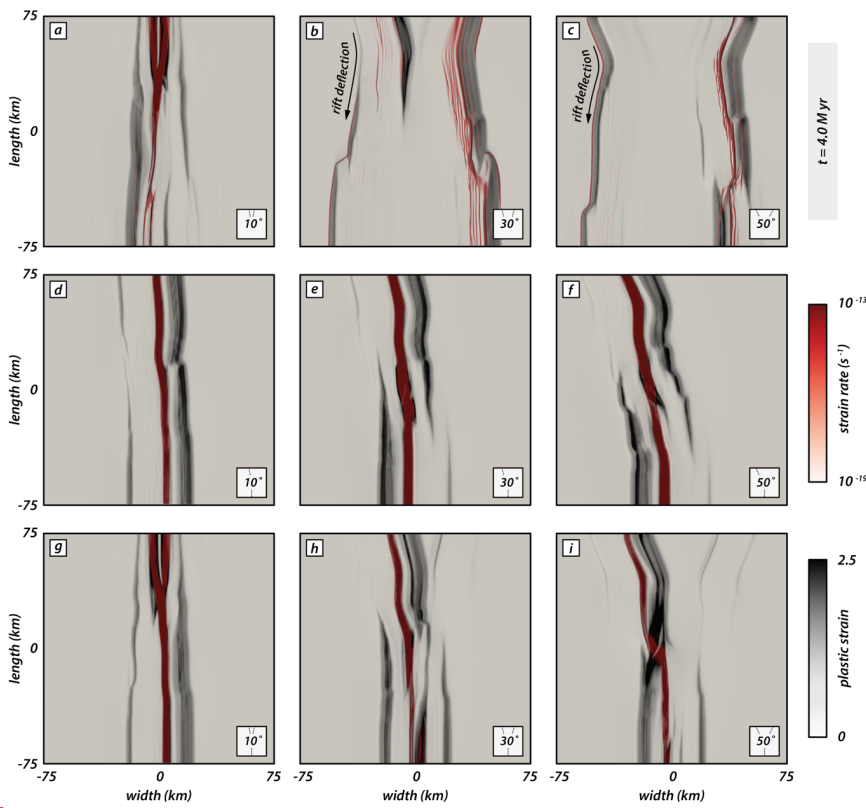
595

596 Models with an i-seed configuration show a continuous and straight rift geometry for all  
597 intermediate angles (fig. 7d-f). For an intermediate angle of 10°, the rift structure is nearly  
598 orthogonal with respect to the extension direction. Note that most plastic strain is  
599 accommodated along the left-dipping rift boundary fault (Fig. 7d). For larger intermediate  
600 angles, the rift subsequently experiences more segmentation with small left stepping  
601 segments towards the rear model part (Fig. 7e,f). Strain accommodation occurs mainly on the  
602 right-dipping rift boundary fault for the frontal model part and switches to the left-dipping  
603 boundary fault in the rear model part.

Deleted: &

Deleted: &



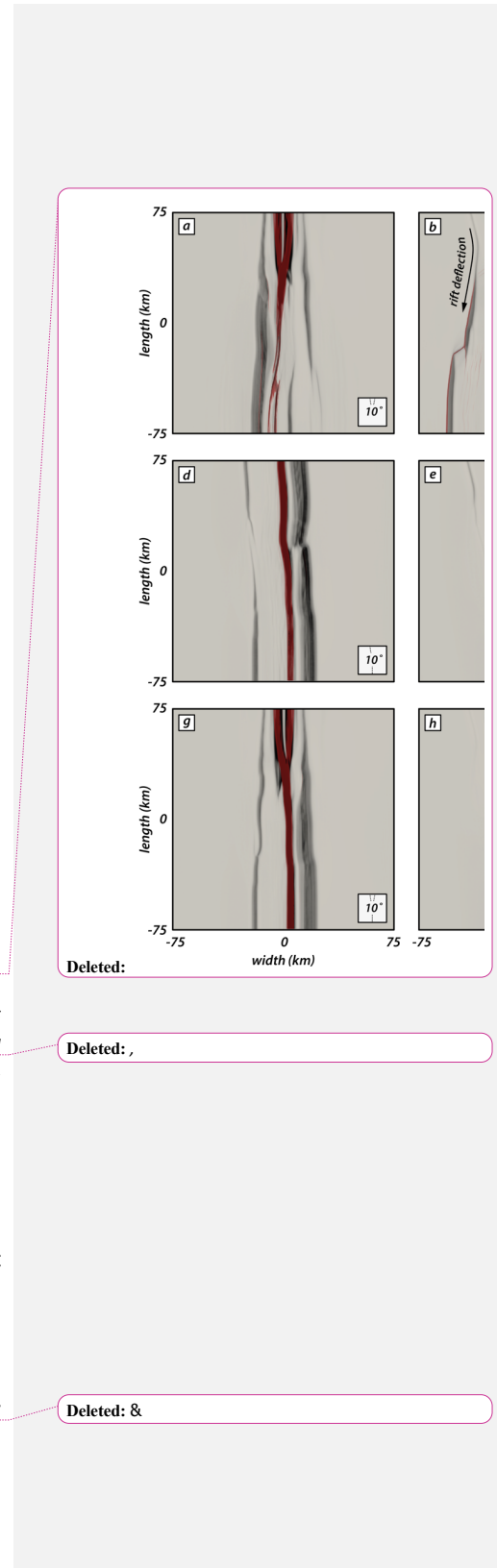


607

608 **Figure 7:** Influence of seed configuration on the final rift geometry after 4 million years. Strain rates (logarithmic) and plastic  
 609 strain are indicated by red and black colors, respectively. a-c) v-seed configuration for intermediate angles of 10°, 30°, and  
 610 50°. d-f) i-seed configuration for intermediate angles of 10°, 30°, and 50°. g-i) y-seed configuration for intermediate angles  
 611 of 10°, 30°, and 50° (reference model).

612

613 The most prominent difference occurs in models with a y-seed configuration and various  
 614 intermediate angles. For an intermediate angle of 10°, the final rift geometry resembles that  
 615 of a continuous straight rift segment (Fig. 7g). Both competing rear seeds are close enough  
 616 such that they build one rift system rather than two distinct branches. For y-seed models with  
 617 a larger intermediate angle (Fig. 7h,i), two individual rear rift segments form and compete for



Deleted:

Deleted: ,

Deleted: &

621 linkage with the frontal rift segment. Plastic strain well illustrates the asymmetric strain  
622 accommodation focused along the left-dipping rift boundary fault of the left rear segment,  
623 whereas the right rear segment only experienced minor strain accommodation (Fig. 7h,i). In  
624 both cases, high strain rates are localized in the axial rift zone and witness activity along the  
625 linked frontal and left rear segments.

Deleted: &

626

627 Note that all experiments with an intermediate angle of  $10^\circ$  (Fig. 7a,d,g) form continuous  
628 straight rift segments, regardless of the seed configuration. Additionally, the final rift geometry  
629 for  $\gamma$ - and  $\nu$ -seed configurations for an intermediate angle of  $10^\circ$  is similar with a gently wider  
630 rift in the frontal model part (Fig. 7a,g). In contrast, for  $i$ -seed configurations the rift width is  
631 similar along the entire length with a minor lateral offset (Fig. 7d). Strain rates are localized  
632 in the axial rift zone throughout the entire model length forking into two close zones in the  
633 rear end where the competing seeds are located.

Deleted: &

Deleted: &

634

### 635 **3.7. $S_{Hmax}$ evolution with progressive deformation**

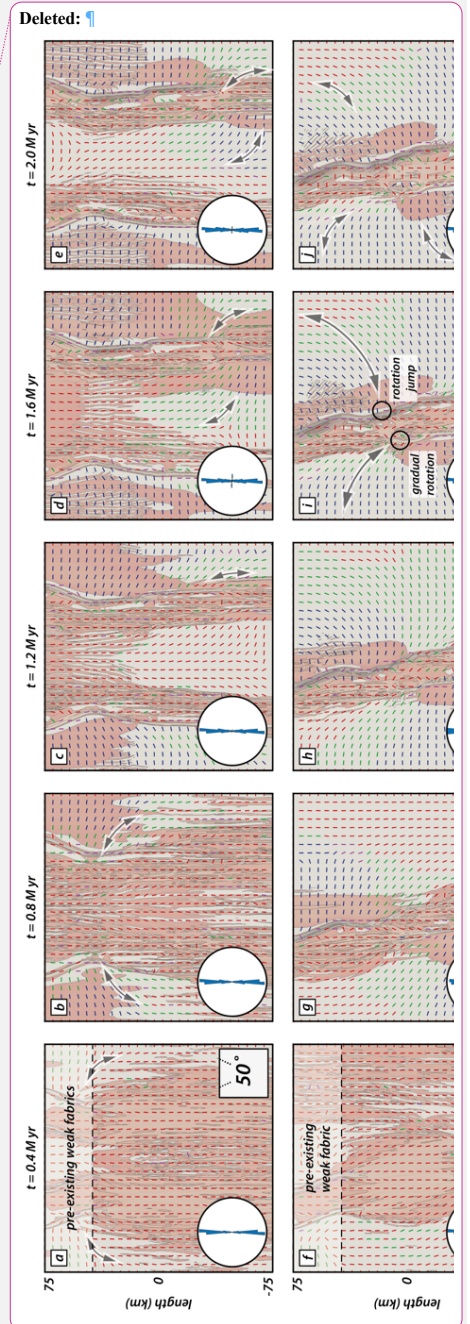
636 In this section we present the distribution and orientation of the maximal horizontal  
637 compressive stress component  $S_{Hmax}$  with progressive rift evolution and segment linkage. We  
638 focus on models with  $\nu$ -,  $i$ -, and  $\gamma$ -seed configurations and an intermediate angle of  $50^\circ$  (Fig.  
639 8; see also supplementary Figures S1-S3) distinguishing between model zones with pre-  
640 existing structures (i.e., weak seeds) and a central zone where material strength is isotropic.

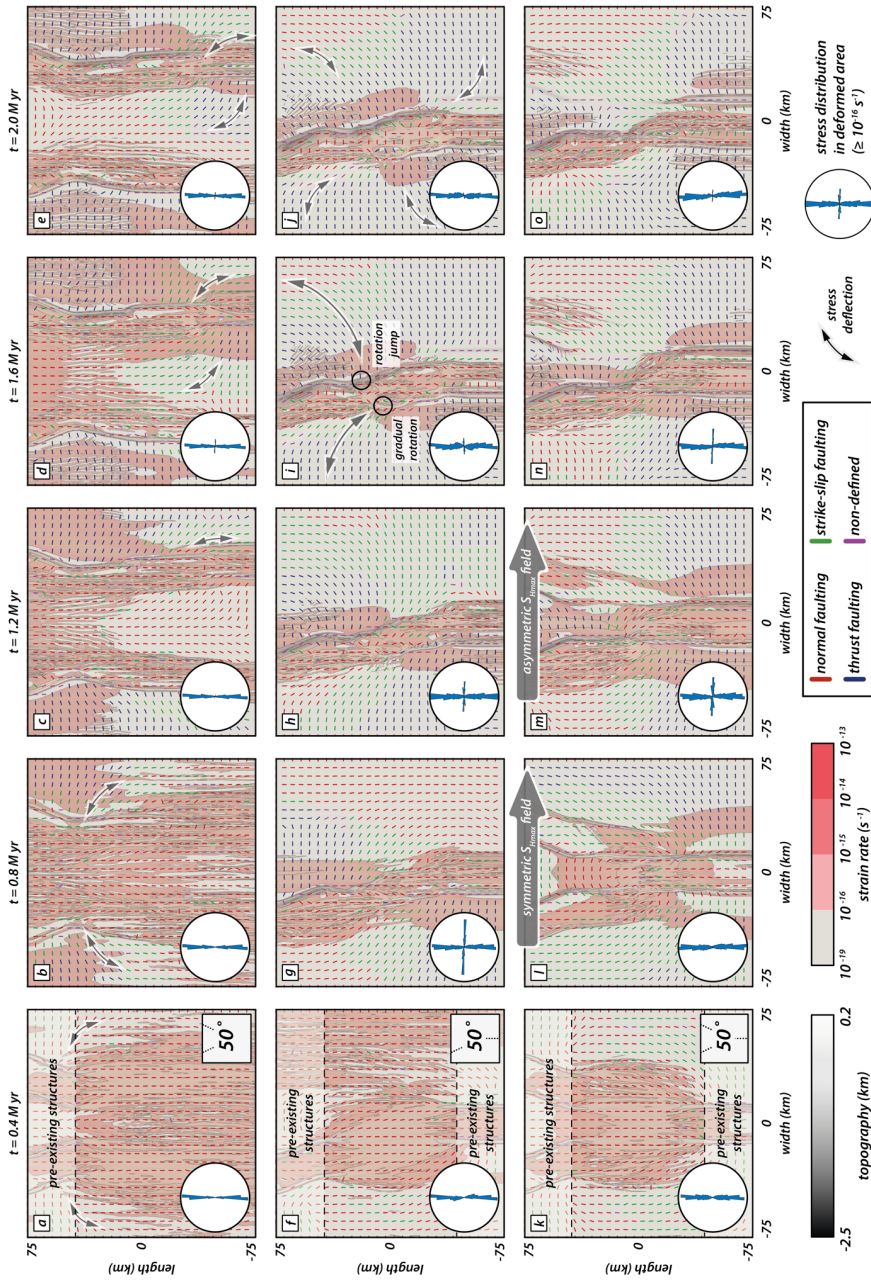
Deleted: weak fabrics

641

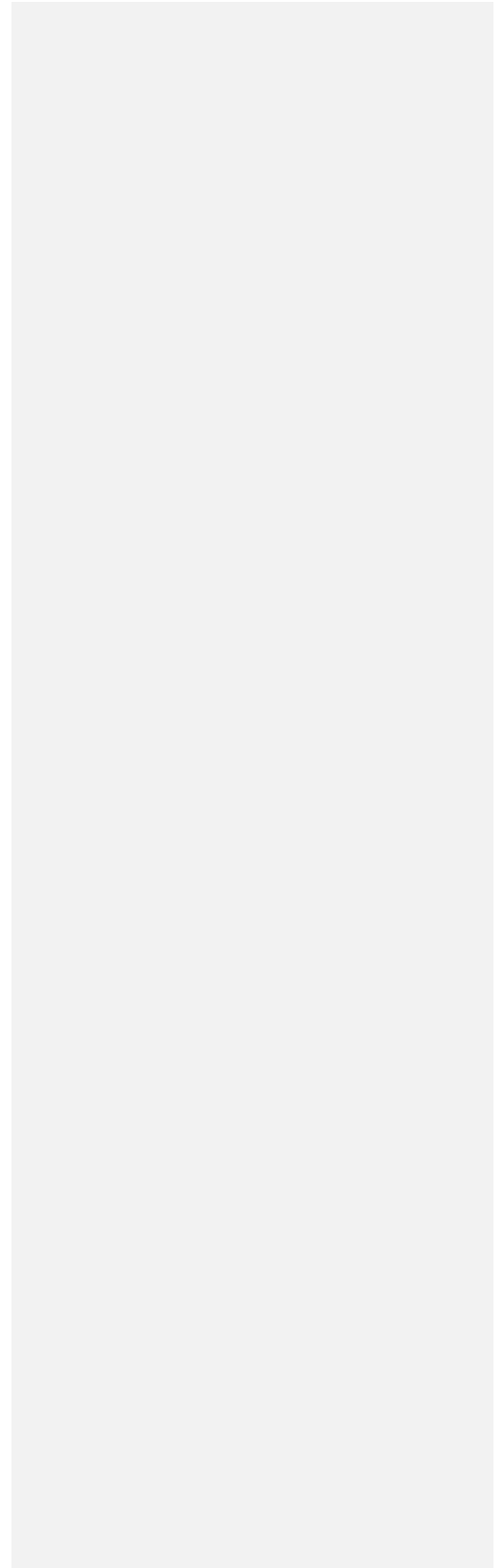
642 Our models depict two distinct phases within the first two million years: early strain  
643 accommodation over a wider model domain followed by strain localization and linkage of  
644 propagating rift segments (see also supplementary Figures S4-S6). Consequently, we focus  
645 on  $S_{Hmax}$  in the first two million years of deformation and its effect on rift propagation. Figure  
646 8 shows the orientation of  $S_{Hmax}$  and the stress regime based on the common color scheme of

651 the World Stress Map (Heidbach et al., 2018). Note that  $S_{Hmax}$  orientation and the stress regime  
652 alone do not suffice to discriminate between locations where stresses exceed crustal strength  
653 and faulting occurs. Strain rate values provide further necessary information, and we use a  
654 threshold of  $10^{-16} \text{ s}^{-1}$  that splits the model into locations of active deformation (i.e.,  $\geq 10^{-16} \text{ s}^{-1}$ )  
655  $^1$ ) and tectonically inactive domains (i.e.,  $< 10^{-16} \text{ s}^{-1}$ ).  
656





660



661 **Figure 8:** Interplay of rift localization and surface stresses. Top views show the distribution of the maximum horizontal  
662 compressive stress component  $S_{Hmax}$  (not scaled to the magnitude) in models with an intermediate angle of  $50^\circ$  at early  
663 deformation stages (i.e., until 2 million years). a-e) v-seed configuration. f-j) i-seed configuration. k-o) y-seed configuration.  
664 Black colors refer to topographic elevation and red colors mark zones where strain rates exceed a threshold of  $10^{-16} s^{-1}$ . Color  
665 coding for the stress regime marks normal, strike-slip, and thrust faulting in red, green, and blue, respectively, using the  
666 common color scheme of the World Stress Map (Heidbach et al., 2018). Elements where the stress regime is non-defined are  
667 marked purple. Black arrows highlight stress deflection of  $S_{max}$ . Rose diagrams show the distribution of  $S_{Hmax}$  orientation in  
668 zones where active faulting occurs (i.e., strain rate  $\geq 10^{-16} s^{-1}$ ). Large grey arrows for the y-seed configuration mark the change  
669 from a symmetric to an asymmetric  $S_{Hmax}$  distribution.

670

### 671 **3.7.1. Effect of $S_{Hmax}$ re-orientation on rift propagation of competing rift** 672 **segments (v-seed models)**

673 Early stages in our numerical experiments are characterized by **rift deflection and** curved fault  
674 traces in the model center where rift segments interact (see Fig. 6). Hereafter we refer to that  
675 phenomenon as arcuate faulting. Arcuate faulting mainly occurs in experiments with larger  
676 intermediate angles ( $>10^\circ$ ) in early stages (Fig. 6), especially if two competing rift segments  
677 are present (v-, and y-seed configurations). Moreover, we have shown that deflection of  
678 propagating rifts occurs when deformation is symmetrically distributed along both competing  
679 rift branches. This is **clearly** visible for the v-seed configuration (Fig. 8a-e). Assuming  
680 orthogonal extension and isotropic material properties,  $S_{Hmax}$  is expected to align perpendicular  
681 to the extension direction producing pure dip-slip normal faults (Anderson, 1905). However,  
682 the model shows an immediate  $S_{Hmax}$  re-orientation at early deformation stages (i.e., after 0.4  
683 million years; Fig. 8a) from a N-S to a E-W orientation in the vicinity of the underlying weak  
684 seeds such that dip slip faults are favored over oblique-slip faults with a strike-slip component.  
685 With progressive extension (Fig. 8b-e),  $S_{Hmax}$  re-orientations successively propagate into the  
686 isotropic zone without pre-existing **structures**, concomitant with the rift propagation.  
687 Consequently, the position of the front where stress rotation occurs propagates over time  
688 resulting in the deflection of the propagating rift arms away from each other.

689

Deleted: well

Formatted: Not Superscript/ Subscript

Formatted: Not Superscript/ Subscript

Deleted: fabrics

692 There is a distinct difference between stress deflection along weak structures and E-W  
693 deflections of  $S_{Hmax}$  in zones where strain rates are below the set threshold of  $10^{-16} s^{-1}$ . The v-  
694 seed configuration shows localized strain accumulation along one rift boundary fault per  
695 segment (i.e., the outer one) resulting in a rift zone with a broad graben system that subsides  
696 (Fig. 8e).  $S_{Hmax}$  re-orientation inside of the graben is in parts identical to the E-W orientation  
697 of  $S_{Hmax}$  outside of the graben. While local  $S_{Hmax}$  rotations may be explained by small  
698 differences in the maximum and intermediate principal stress components, such E-W stress  
699 re-orientation in our model occurs systematically and suggest that this feature reflects the  
700 influence of the strength anisotropy (Morley, 2010). The initial  $S_{Hmax}$  deflection near weak  
701 structures locally favors dip-slip faulting but also has regional influence on the overall stress  
702 regime.

Deleted: fabrics

Deleted: fabrics

703

### 704 **3.7.2. $S_{Hmax}$ evolution in sub-parallel rift segments (i-seed models)**

Deleted: subparallel

705 During the early stage (i.e., after 0.4 million years, Fig. 8f), the distribution of  $S_{Hmax}$  resembles  
706 the distribution from the v-seed configuration described in the previous section. Stress  
707 deflection mainly occurs in zones where a weak fabric is present.  $S_{Hmax}$  values in the central  
708 zone rotate by a small amount and reflect arcuate faulting (see Fig. 6). Since the two rift  
709 segments propagate in opposing directions, linkage is efficient and localizes in a short time  
710 (Fig. 8f-j).  $S_{Hmax}$  values deflect accordingly along propagating faults, which affects the entire  
711 model domain. This deflection does not occur symmetrically on both sides of each rift segment.  
712 Rather, it shows two distinct zones: 1) E-W orientations outside the rift deflect into a parallel  
713 orientation near the rift boarder or 2) N-S orientations outside of the rift deflect into E-W  
714 orientations near faults (Fig. 8j).

715

716 We find that  $S_{Hmax}$  orientations deflect gradually from E-W to N-S along abandoned rift  
717 boundary faults where activity ceased (Fig. 8h-j; upper left and lower right model domain). In



721 contrast,  $S_{Hmax}$  re-orientations from N-S to nearly E-W towards active rift boundary faults are  
722 followed by a rapid flip back to N-S along the faults (Fig. 8h-j; lower left and upper right model  
723 domain). The two types of re-orientation seem to correspond with two types of deformed  
724 zones. Where deformation is strongly localized along rift boundary faults, jumps in the  $S_{Hmax}$   
725 orientation occur. In contrast, zones where inward migration of fault activity activates intra-  
726 rift faults,  $S_{Hmax}$  re-orientation occurs gradually.

727

### 728 **3.7.3. Rift arm competition and deflection (y-seed models)**

729 A prominent feature in our models with two competing rift segments is the deflection of rift  
730 branches and arcuate strain rate patterns (Fig. 8a-e) in the model with a v-seed configuration.  
731 Moreover, the i-seed configuration demonstrates a gradual  $S_{Hmax}$  re-orientation over a broader  
732 pre-weakened zone due to formerly active boundary faults. One could therefore expect that  
733 both features should occur in the model with y-seed configuration (Fig. 8k-o).

734

735 Indeed, early stages (i.e., after 0.4 million years; Fig. 8k) are characterized by a symmetric  
736 stress field with re-oriented  $S_{Hmax}$  values near the two rear rift segments. However, in contrast  
737 to the v-seed configuration,  $S_{Hmax}$  re-orientation also occurs near the frontal pre-existing weak  
738 fabric along developing rift boundary faults. In the isotropic zone,  $S_{Hmax}$  values dominantly  
739 show a N-S direction. The general N-S orientation reflects the regional stress field due to an  
740 E-W extension as predicted by Anderson (1905) in isotropic areas, into which rift segments  
741 have yet to propagate. With ongoing extension, all three rift segments propagate into the  
742 isotropic zone and cause a re-orientation of  $S_{Hmax}$  (Fig. 8l). Note that after 0.8 million years  
743 the stress re-orientation occurs symmetrically. This contrasts with the i-seed configuration  
744 where  $S_{Hmax}$  values deflect into either, an E-W orientation along active rift boundary faults or  
745 gradually turn into a fault parallel direction over a broader weakened zone (see subsection  
746 3.7.2.). The early symmetric stress distribution in the y-seed configuration model is

Formatted

Deleted: Figs

Formatted: Not Superscript/ Subscript

Deleted: where

Deleted: not

Deleted: propagated into

Deleted: into



752 unarguably due to the symmetric seed configuration (see also Fig. 8a-e). At this stage, dip-  
753 slip faulting along the competing sub-parallel rift segments is favored over oblique slip faults  
754 as in models with a v-seed configuration. It is only after 1.2 million years, when fault activity  
755 along the right rear segment ceases that deformation localizes along the left rear and frontal  
756 segments and linkage intensifies (Fig. 8m). Successively, localization and linkage occur  
757 coevally with a switch from a symmetric to an asymmetric stress distribution and resembles  
758 more the stress distribution in the i-seed configuration model (Fig. 8f-j). The model state after  
759 1.2 million years (Fig. 8m) also marks the switch from a symmetric to an asymmetric stress  
760 distribution that was formerly dominated by the competing rear rift segments with dip-slip  
761 faulting favored along the two competing rift segments (see also v-seed configuration; Fig. 8  
762 a-e). After 1.2 million years the system is dominated by the linkage of two obliquely oriented  
763 segments (i.e., i-seed configuration). Note that after 1.2 million years dip-slip faulting mostly  
764 occurs along the competing rift segment that links with the opposingly propagating segment  
765 whereas dominantly oblique slip faults occur along the abandoned rift segment where activity  
766 ceases.

Deleted: fig

Deleted: (i.e.,

Deleted: ) whereas after

Formatted: Strikethrough

767  
768 The symmetry switch is also visible in rose diagrams of stress orientations within the active  
769 faulting zone (i.e., strain rate  $\geq 10^{-16} \text{ s}^{-1}$ ). A dominantly N-S oriented  $S_{Hmax}$  distribution changes  
770 to a bimodal distribution with a second E-W orientation (Fig. 8l-n). Similarly, bimodal  $S_{Hmax}$   
771 distribution is also visible in the experiment with an i-seed configuration but occurs earlier.  
772 Since the experiment with an i-seed configuration is never in the state of an early symmetric  
773 stress distribution linkage is facilitated and occurs earlier (Fig.8g-i).

Deleted: This

Deleted: a

Deleted: a

Deleted: .....

#### 775 **4. Discussion**

776 Despite the relatively simple setup of our experiments, the interaction of individual weak seeds  
777 generates a complex evolution of linkage patterns. In the following we discuss the effect of

785 pre-existing structures on  $S_{Hmax}$  re-orientations and how, in return, stress re-orientation  
786 influences rift propagation and rift segment linkage.

Deleted: fabrics

787

788 **4.1. Effect of pre-existing structures on rift segment propagation,**  
789 **interaction, and  $S_{Hmax}$**

Deleted: fabrics

790 Previous modelling studies demonstrated that pre-existing weaknesses may cause local re-  
791 orientations of  $S_{Hmax}$  resulting in extensional faults with an oblique orientation to the regional  
792 extension direction which exhibit pure dip-slip behavior (e.g., Morley, 2010; Corti et al., 2013;  
793 Morley, 2017; Philippon et al., 2015). This contrasts the expected (assuming Andersonian  
794 faulting theory) occurrence of faults with an oblique slip component above pre-existing

Deleted: , 2010

795 structures that are obliquely oriented with respect to the extension direction (Tron and Brun,  
796 1991; Withjack and Jamison, 1986). Our  $S_{Hmax}$  analysis documents two types of stress re-  
797 orientation, either gradually or by a jump along faults (Fig. 8i). A potential explanation for the  
798 two types of stress deflection is that cessation of boundary fault activity (and subsequent  
799 faulting activity along intra-rift faults) creates a broad zone of reduced crustal strength. Hence,  
800  $S_{Hmax}$  orientations successively re-orient along those formerly active faults and eventually  
801 rotate into a N-S orientation along active intra-rift faults. In contrast, where faulting activity  
802 is strongly localized along rift boundary faults, re-orientation occurs rapidly by a jump from E-  
803 W to a N-S orientation. This suggests that formerly active faults act as a wider zone of pre-  
804 weakened material, where stresses deflect sequentially rather than with a rapid jump. Similar  
805 observations have been made in previous studies of numerical models (Gudmundsson et al.,  
806 2010; Kattenhorn et al., 2000). These experiments suggest that earlier fractures lead to  
807 subzones (within a broader damage zone), where stresses subsequently rotate away from the  
808 regional stress field. Although our analog and numerical models do not feature elastic  
809 deformation, they indicate that stress deflection is an ongoing process, even after elastic  
810 material failure. Such a stress deflection further implies that stress orientations in rocks with

Deleted: fabrics

815 pre-existing weaknesses can substantially deviate from predicted orientations in isotropic  
816 media (Anderson, 1905).

817

818 It has been proposed that early faulting and propagation in the Rukwa and North Malawi Rifts  
819 (Fig. 1c) were guided by pre-existing basement fabrics (Heilman et al., 2019). This region is  
820 further shaped by a flip in the boundary fault polarity in the present-day geometry within the  
821 interaction zone between Rukwa Rift and North Malawi Rift (Bosworth, 1985). Our i-seed

822 models show identical geometries for increasing intermediate angles (Figs. 7h,i and S5), where  
823 plastic strain near pre-existing structures is mostly accommodated along prominent rift

824 boundary faults that flip fault polarity from the frontal to the rear rift segment. This flip in  
825 fault polarity occurs prominently in models with an intermediate angle  $\geq 10^\circ$ . We speculate  
826 that the increasing obliquity of the southward propagating rift segment favors asymmetric  
827 graben evolution with one dominant boundary fault accommodating a larger amount of strain.  
828 In contrast to small intermediate angles (i.e.,  $10^\circ$ ), seed configurations with a higher obliquity  
829 provoke local rotation of  $S_{Hmax}$  within the interaction zone into a strike-slip regime near the  
830 subordinate boundary fault (Fig. S5). Hence, strain accommodation along incipient faults  
831 within the dip-slip regime is favored. This facilitates propagation along those dominant rift  
832 boundary faults and eventually defines the final rift geometry.

833

834 Kolawole et al. (2018) further propose two different types of strain accommodation at early  
835 rift phases. Prominent strain accommodation localized onto a discrete and narrow zone along  
836 large rift boundary faults (Style-1; sensu Kolawole et al., 2018) and faulting distributed over  
837 a broader zone, where fault clusters may reflect pre-conditioning of the material (Style-2;  
838 sensu Kolawole et al., 2018). With this perspective, jumps and gradual rotation of  $S_{Hmax}$   
839 orientations are comparable to Style-1 and Style-2 strain localization, respectively, as  
840 proposed by Kolawole et al. (2018). Hence, the type of weakness (narrow discrete zone or

Deleted: (

Deleted: ).

Deleted: Fig

Deleted: &

Deleted: weak fabrics

846 distributed cluster zone) should also be reflected by the stress re-orientation distribution  
847 (Morley, 2010).

Deleted: broad discrete

848

#### 849 **4.2. Local $S_{Hmax}$ re-orientation and its influence on rift segment interaction** 850 **and rift deflection**

851 A particular observation in our experiments with a v-, and y-seed configuration is that two  
852 sub-parallel rift segments, which propagate approximately in the same direction deflect away  
853 from each other at early stages. This is somewhat surprising as one would expect the two rift  
854 segments to cut towards each other by minimizing fault length. The occurrence of rift  
855 deflection in both analog and numerical experiments validates that the results are robust and  
856 require discussing the role of  $S_{Hmax}$  re-orientation and how it influences rift segment  
857 interaction.

858

859 We speculate that, while both rear rift segments in our y-seed models equivalently  
860 accommodate strain in the early stages (i.e., when the overall stress distribution is symmetric;  
861 Fig. 8),  $S_{Hmax}$  orientations are dominated by the influence of the two competing rear rift  
862 segments that accommodate strain in equal parts. It is only after fault activity along one rear  
863 segment ceases that deformation localizes along the active rear and frontal segments and  
864 linkage intensifies. Strain localization and linkage occur coevally with a switch from a  
865 symmetric to an asymmetric stress distribution resembling the stress distributions in v-, and  
866 i-seed configuration models, respectively. The switch from a symmetric to an asymmetric  
867 stress distribution in y-seed models also marks the switch from a system that was formerly  
868 dominated by the competing rear rift segments (i.e., v-seed configuration) to a system that  
869 is dominated by the linkage of two obliquely oriented segments (i.e., i-seed configuration).

870

872 In models with a v-seed configuration, however, the symmetric phase prevails and causes  
873 coeval  $S_{Hmax}$  re-orientations and rift deflection that cause divergence of the two propagating  
874 rift segments. A similar process of extensional segment interaction via stress rotation is known  
875 from mid-ocean ridge settings: Pollard and Aydin (1984) argue that paths of two opposingly  
876 propagating oceanic ridges weakly diverge due to shear stresses that divert propagating ridges  
877 as they approach each other. Once the two ridges overlap, the stress field changes causing  
878 convergence and intersection. Similarly, Nelson et al. (1992) describe interference of  
879 compressional zones of propagating cracks diverting their tips before they overlap and turn  
880 back toward another. In this respect, our models with a v-seed configuration suggest that  
881 stresses also cause divergence of two rift segments that propagate approximately in the same  
882 direction. However, overlap never occurs (as they propagate approximately in the same  
883 direction) and hence, the two segments remain in a stress field that further diverts their paths.

884  
885 Only in models with a y-seed configuration, compressional zones and rift deflection can be  
886 overcome once the opposingly propagating rift segment links with one of the competing rift  
887 segments. Linkage occurs after about the first million years, concurrently with rift deflection  
888 and abandonment of the right rear segment (Figs. 9a and S6). Moreover, remaining activity

889 in the right rear segment depicts low strain rates along numerous arcuate intra-rift faults (Figs.  
890 9b and S6). This suggests that linkage and rift abandonment are closely coupled and faulting  
891 along the linked segments intensifies when the activity along the remaining rift segment

892 ceases. In addition, the left rear segment displays a rather asymmetric half graben geometry  
893 (Figs. 5c,d, 7i and S4) with one prominent rift boundary fault accommodating a larger part of  
894 plastic strain similar to our models with a i-seed configuration (see also Figs. 7e,f and S5).  
895 Dominant strain accommodation occurs along the west-dipping rift boundary fault of the left  
896 rear segment coinciding with jumps in the  $S_{Hmax}$  orientation (Fig. 8m-o). Our modelling results

897 show that stress deflection along rift segment tips is a mechanical consequence of the

Deleted: Fig. 9b

Deleted: Fig. 9c

Deleted: With respect to the Turkana Region this suggests that the KSFB may represent a southward propagating rift branch that experienced a limited amount of extension-related deformation before propagation aborted, similar to the neighboring Ririba Rift in the east (Corti et al., 2019). The definite linkage of the Ethiopian and Kenyan Rift via the lake Turkana basin may represent a switch from a symmetric to an asymmetric stress distribution after which local stress re-orientation favored increased faulting activity along the linked system and caused the abandonment of the young KSFB as seen in our models (Fig.9).

912 interaction between weak zones and far-field stresses offering a potential explanation for  
913 naturally occurring rift deflection. However, we must emphasize that complexities in natural  
914 rift settings pose additional difficulties that require further investigations of stress orientations.

915

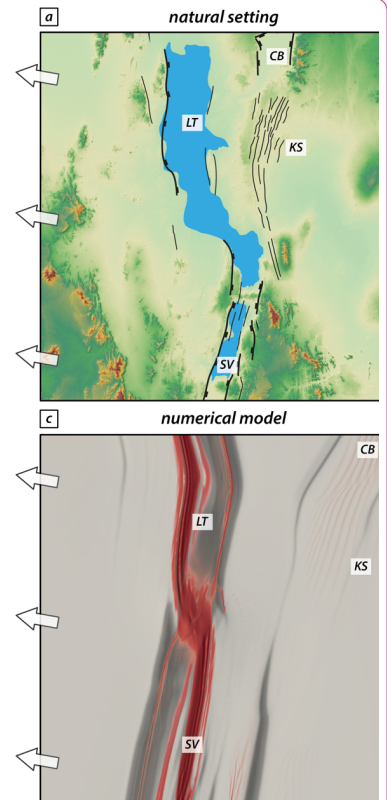
916 An example of rift deflection *in nature* has been described in the Main Ethiopian Rift.  
917 Geophysical and geologic studies evidence that pre-existing structures controlled the  
918 approximately 11 Ma southward propagation of the Northern Main Ethiopian Rift and its  
919 contemporaneous westward deflection along the Yerer-Tullu Wellel Volcanotectonic  
920 Lineament (YTVL; Abebe et al., 1998; Keranen and Klemperer, 2008; Muhabaw et al., 2022).  
921 Only after the rotation of the principal stress direction at about 5-6 Ma (Bonini et al., 2005),  
922 extension along the YTVL ceased and deformation localization along the Central Main  
923 Ethiopian Rift became more favorable. Our models document similar rift deflections and  
924 moreover indicate that, even in the absence of changing plate motions, rift segments deflect,  
925 and may cease while competing rift segments prevail and strain further localizes.

926

927 For the Canyonlands National Park, it has been proposed that it is mainly the lateral offset  
928 between pre-existing structures that explains the diversity of structures (Allken et al., 2013;  
929 Fig. 1d). With larger offsets, interaction between adjacent rift segments is limited and  
930 competing grabens persist and endure ongoing propagation coevally. We find that stresses,  
931 in combination with the geometry of pre-existing structures, play an important role and that  
932 they have a mutual effect on one another. Hence, stress distribution must be considered as  
933 an important factor especially in early rifting stages when segments link and predetermine  
934 strain localization *during subsequent progressive rifting*.

935

Deleted: such as seen in the KSFB.



Deleted:

Figure 9: Summary plot showing the geometric similarity of rift segment linkage, deflection of competing branches and abandonment in natural setting, analog, and numerical models. a) Major rift segments in the Lake Turkana Rift system with a double-armed rift system. CB: Chew Bahir basin; LT: Lake Turkana basin; KS: Kino Sogo Fault Belt; SV: Suguta Valley. b) Observed key features at the final stage of the analog model. c) Final strain and strain rate pattern in the numerical reference model. d) Conceptual interpretation of the Lake Turkana Rift based on our numerical results (for details see text).

Another

Deleted: somewhat

Deleted: 1b

Deleted: in following

Deleted: phases

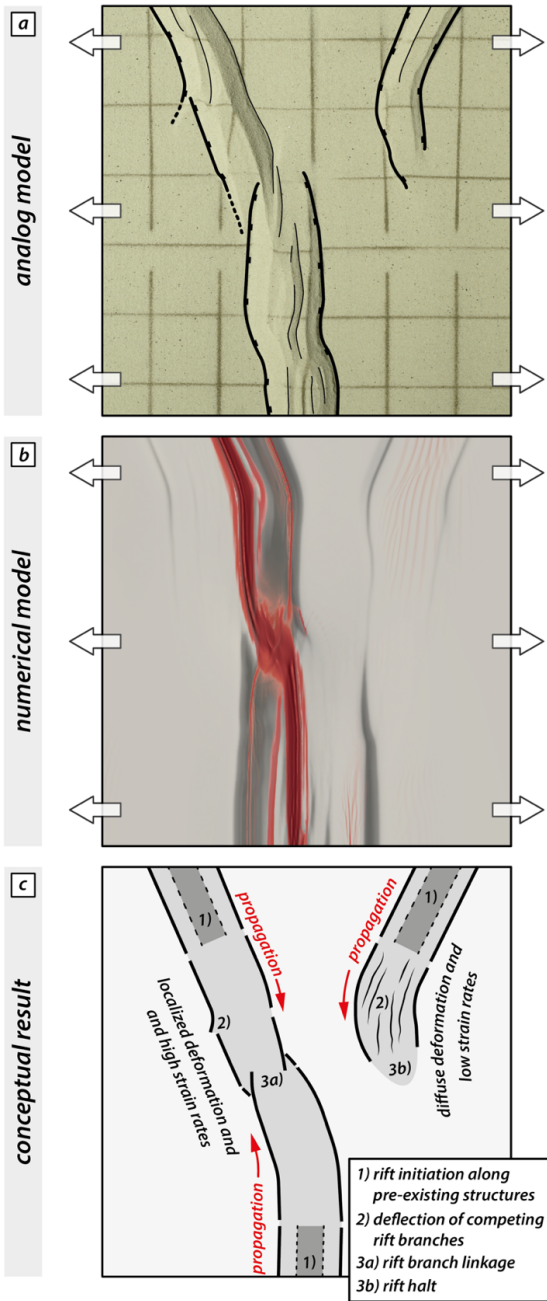


Figure 9: Summary plot showing the geometric similarity of rift segment linkage, deflection of competing branches and abandonment in analog and numerical models. a) Observed key features at the final stage of the analog model. b) Final strain and strain rate pattern in the numerical reference model. c) Conceptual interpretation of rift deflection and linkage based on our analog and numerical results (for details see text).

957 **5. Conclusions**

958 We present a series of analog and numerical rifting experiments. Our results suggest that,  
959 even in a relatively simple iso-viscous two-layer crustal setup, pre-existing weaknesses  
960 substantially disturb the regional stress pattern, which impacts rift propagation and the overall  
961 rift evolution. The complex stress re-orientation is distinct for different seed configurations  
962 (i.e., v-seed, i-seed, and y-seed) and closely interacts with the final rift geometry. The most  
963 important findings of our study can be summarized as follows:

964

965 • Our numerical experiments reproduce rift segment deflection seen in our analog  
966 models. This highlights the robustness of our results and their applicability to  
967 interpreting rift segment propagation, interaction, and linkage in natural settings of  
968 continental rifting.

969 • Pre-existing structures may control localization of rift segments that successively  
970 propagate into previously undeformed areas. Consequently, stress re-orientation  
971 initially occurs along pre-conditioned zones and propagates, coevally with rift segment  
972 propagation and strain accrual, into formerly undeformed areas.

973 • Interacting stresses between two competing rift segments may cause outward  
974 deflection of the propagating rift tips resulting in a successively broader rift geometry  
975 along-strike.

976 • Outward deflection of competing rift segments is less prominent if an opposingly  
977 propagating rift segment is present. With progressive extensional deformation, strain  
978 accrual along one of the competing rift segments prevails whilst faulting activity along  
979 the other segment ceases. Coevally, the general stress orientation changes from a  
980 symmetric to an asymmetric distribution indicating the onset of rift linkage.

981 • Our modelling results reproduce first-order structures of natural examples from the  
982 East African Rift System and, on smaller scale, graben structures in the Canyonlands

Deleted: fabrics



984 National Park. The combined investigation of surface stresses and strain localization  
985 provides an explanation for distinct rift deflection among competing rift segments and  
986 rift linkage structures where ongoing deformation and stresses mutually affect each  
987 other.

988

989 While changes in rift orientation are often used to infer regional palaeo-movements, we  
990 demonstrate that local stress field re-orientations can occur under constant plate motions.

Formatted: Justified, Line spacing: Double

991 ~~Albeit on a smaller scale, implications from our observations corroborate findings from~~  
992 ~~previous studies (Brune; 2014; Duclaux et al., 2020; Gapais et al., 2000). Locally, stress and~~  
993 ~~strain can largely deviate from a regional, far-field pattern and instead represent local~~  
994 ~~deformation interference. In addition, the~~ observed stress re-orientations change over time  
995 indicating that stresses measured in natural examples may depict transient stages that change  
996 with progressive deformation due to subsequent changes in material strengths. ~~(Morley et al.,~~  
997 ~~2004). This implication must be considered in processing local fault-slip data when interpreting~~  
998 ~~the evolution of rifts at any scale.~~

Deleted: The

Deleted: . ¶

1001 **Data availability**

1002 Rheological measurements of the used analog materials are available in the form of open  
1003 access data publications provided by the GFZ Data Service (brittle materials: Schmid et al.,  
1004 2020a; Schmid et al., 2020b; viscous materials: Zwaan et al., 2018).

1005

1006 **Acknowledgements**

1007 We thank Esther Heckenbach for helpful assistance with post processing and visualization.  
1008 The work was supported by the North-German Supercomputing Alliance (HLRN). We thank  
1009 the Swiss National Science Foundation for providing financial support. Finally, we thank the  
1010 two reviewers, Guillaume Duclaux and Chris Morley for their detailed, constructive and  
1011 motivating comments that significantly helped to improve this manuscript.

1012

1013 **Funding**

1014 This project is supported by the Swiss National Science Foundation [grant number  
1015 200021\_178731].

1016

1017 **CRedit authorship contribution statement**

1018 Timothy C. Schmid: Conceptualization, Methodology, Investigation, Formal Analysis, Writing  
1019 – original draft, Visualization, Data curation. Sascha Brune: Conceptualization, Methodology,  
1020 HPC funding acquisition, Supervision, Project administration, Writing – review & editing. Anne  
1021 Glerum: Methodology, Software, HPC funding acquisition, Writing – review & editing. Guido  
1022 Schreurs: Writing – review & editing, Supervision, Project administration, Funding acquisitions,

1023 Resources.

1024

Deleted: **Competing interests**  
The authors declare that they have no conflict of interest.

Deleted: .....Page Break.....

1030

## References

1031 Abebe, T., Mazzarini, F., Innocenti, F., and Manetti, P.: The Yerer-Tullu Wellel volcanotectonic lineament: A  
1032 transensional structure in central Ethiopia and the associated magmatic activity, *Journal of African Earth Sciences*,  
1033 **26**, 135-150, 1998.  
1034 [https://doi.org/10.1016/S0899-5362\(97\)00141-3](https://doi.org/10.1016/S0899-5362(97)00141-3)  
1035  
1036 Acocella, V., Faccenna, C., Funicello, R., and Rossetti, F.: Sand-box modelling of basement-controlled transfer  
1037 zones in extensional domains, *Terra Nova-Oxford*, **11**, 149-156, 1999.  
1038  
1039 Adam, J., Urai, J., Wieneke, B., Oncken, O., Pfeiffer, K., Kukowski, N., Lohrmann, J., Hoth, S., Van Der Zee, W.,  
1040 and Schmatz, J.: Shear localisation and strain distribution during tectonic faulting—New insights from granular-  
1041 flow experiments and high-resolution optical image correlation techniques, *Journal of Structural Geology*, **27**, 283-  
1042 301, 2005.  
1043 <https://doi.org/10.1016/j.jsg.2004.08.008>  
1044  
1045 Allken, V., Huismans, R. S., and Thieulot, C.: Three-dimensional numerical modeling of upper crustal extensional  
1046 systems, *Journal of Geophysical Research: Solid Earth*, **116**, 2011,  
1047 <https://doi.org/10.1029/2011JB008319>  
1048  
1049 Allken, V., Huismans, R. S., and Thieulot, C.: Factors controlling the mode of rift interaction in brittle-ductile coupled  
1050 systems: A 3D numerical study, *Geochemistry, Geophysics, Geosystems*, **13**, 2012,  
1051 <https://doi.org/10.1029/2012GC004077>  
1052  
1053 [Allken, V., Huismans, R. S., Fossen, H., and Thieulot, C.: 3D numerical modelling of graben interaction and linkage:  
1054 a case study of the Canyonlands grabens, Utah, \*Basin Research\*, \*\*25\*\*, 436-449, 2013.  
1055 <https://doi.org/10.1111/bre.12010>  
1056  
1057 Anderson, E. M.: The dynamics of faulting, \*Transactions of the Edinburgh Geological Society\*, \*\*8\*\*, 387-402, 1905,  
1058 <https://doi.org/10.1144/transed.8.3.387>  
1059  
1060 Bellahsen, N., and Daniel, J. M.: Fault reactivation control on normal fault growth: an experimental study, \*Journal  
1061 of Structural Geology\*, \*\*27\*\*, 769-780, 2005,  
1062 <https://doi.org/10.1016/j.jsg.2004.12.003>  
1063  
1064 Bonini, M., Corti, G., Innocenti, F., Manetti, P., Mazzarini, F., Abebe, T., and Pecskey, Z.: Evolution of the Main  
1065 Ethiopian Rift in the frame of Afar and Kenya rifts propagation, \*Tectonics\*, \*\*24\*\*, 2005,  
1066 <https://doi.org/10.1029/2004TC001680>  
1067  
1068 Bosworth, W.: Geometry of propagating continental rifts, \*Nature\*, \*\*316\*\*, 625-627, 1985,  
1069 <https://doi.org/10.1038/316625a0>  
1070  
1071 Brune, S.: Evolution of stress and fault patterns in oblique rift systems: 3-D numerical lithospheric-scale  
1072 experiments from rift to breakup, \*Geochemistry, Geophysics, Geosystems\*, \*\*15\*\*, 3392-3415, 2014,  
1073 <https://doi.org/10.1002/2014GC005446>  
1074  
1075 Brune, S., and Autin, J.: The rift to break-up evolution of the Gulf of Aden: Insights from 3D numerical lithospheric-  
1076 scale modelling, \*Tectonophysics\*, \*\*607\*\*, 65-79, \[10.1016/j.tecto.2013.06.029\]\(https://doi.org/10.1016/j.tecto.2013.06.029\), 2013,  
1077 <https://doi.org/10.1016/j.tecto.2013.06.029>  
1078  
1079 Brune, S., Corti, G., and Ranalli, G.: Controls of inherited lithospheric heterogeneity on rift linkage: Numerical and  
1080 analog models of interaction between the Kenyan and Ethiopian rifts across the Turkana depression, \*Tectonics\*,  
1081 \*\*36\*\*, 1767-1786, 2017,  
1082 <https://doi.org/10.1002/2017TC004739>  
1083  
1084 Brune, S., Popov, A. A., and Sobolev, S. V.: Modeling suggests that oblique extension facilitates rifting and  
1085 continental break-up, \*Journal of Geophysical Research: Solid Earth\*, \*\*117\*\*, 2012,  
1086 <https://doi.org/10.1029/2011JB008860>  
1087  
1088 Childs, C., Watterson, J., and Walsh, J.: Fault overlap zones within developing normal fault systems, \*Journal of the  
1089 Geological Society\*, \*\*152\*\*, 535-549, 1995,  
1090 <https://doi.org/10.1144/gsjgs.152.3.0535>  
1091](https://doi.org/10.1111/bre.12010)

Deleted: ¶

Deleted: ., 1998.

Formatted ... [1]

Formatted ... [2]

Deleted: *Journal of African Earth Sciences* 26, 135-150.¶

Formatted ... [3]

Formatted ... [4]

Formatted ... [5]

Deleted: ., 1999.

Formatted ... [6]

Formatted ... [7]

Deleted: *Terra Nova-Oxford* 11, 149-156.¶

Formatted ... [8]

Deleted: ., 2005.

Formatted ... [9]

Formatted ... [10]

Deleted: *Journal of Structural Geology* 27, 283-301.¶

Formatted ... [11]

Moved down [11]: Fossen, H.,

Deleted: ., 2013. 3D

Deleted: modelling

Deleted: graben interaction and linkage: a case study

Formatted ... [12]

Formatted ... [13]

Formatted ... [14]

Formatted ... [15]

Deleted: the Canyonlands grabens, Utah

Formatted ... [16]

Formatted ... [17]

Moved down [12]: <https://doi.org/10.1111/bre.12010>

Moved down [13]: Allken, V., Huismans, R.

Deleted: *Basin Research* 25, 436-449.¶

Deleted: S., Thieulot, C., 2011. Three-dimensiona... [19]

Formatted ... [18]

Formatted ... [20]

Deleted: ., 2012.

Formatted ... [21]

Formatted ... [22]

Deleted: *Geochemistry, Geophysics, Geosystems* 13.¶

Formatted ... [23]

Moved (insertion) [13] ... [24]

Formatted ... [25]

Moved (insertion) [12]

Formatted ... [28]

Formatted ... [26]

Field Code Changed ... [27]

Deleted: ., 1905.

Deleted: .¶

Formatted ... [29]

Formatted ... [30]

Formatted ... [31]

Formatted ... [32]

Formatted ... [33]

Formatted ... [34]

Deleted: .,

Deleted: ., 2005.

Formatted ... [35]

Formatted ... [36]

Deleted: *Journal of Structural Geology* 27, 769-780.¶

Formatted ... [37]

Formatted ... [38]

Deleted: ., 2005.

Formatted ... [39]

1184 Collanega, L., Jackson, C. A.-L., Bell, R., Coleman, A. J., Lenhart, A., and Breda, A.: How do intra-basement fabrics  
1185 influence normal fault growth? Insights from the Taranaki Basin, offshore New Zealand, 2018,  
1186 <https://doi.org/10.31223/osf.io/8rn9u>

1187  
1188 Corti, G.: Evolution and characteristics of continental rifting: Analog modeling-inspired view and comparison with  
1189 examples from the East African Rift System, *Tectonophysics*, 522-523, 1-33, 10.1016/j.tecto.2011.06.010, 2012,  
1190 <https://doi.org/10.1016/j.tecto.2011.06.010>

1191  
1192 Corti, G., van Wijk, J., Cloetingh, S., and Morley, C. K.: Tectonic inheritance and continental rift architecture:  
1193 Numerical and analogue models of the East African Rift system, *Tectonics*, 26, 2007,  
1194 <https://doi.org/10.1029/2006TC002086>

1195  
1196 Corti, G., Philippon, M., Sani, F., Keir, D., and Kidane, T.: Re-orientation of the extension direction and pure  
1197 extensional faulting at oblique rift margins: Comparison between the Main Ethiopian Rift and laboratory  
1198 experiments, *Terra Nova*, 25, 396-404, 2013,  
1199 <https://doi.org/10.1111/ter.12049>

1200  
1201 Corti, G., Cioni, R., Franceschini, Z., Sani, F., Scaillet, S., Molin, P., Isola, I., Mazzarini, F., Brune, S., and Keir, D.:  
1202 Aborted propagation of the Ethiopian rift caused by linkage with the Kenyan rift, *Nature communications*, 10, 1-  
1203 11, 2019,  
1204 <https://doi.org/10.1038/s41467-019-09335-2>

1205  
1206 Crameri, F., Shephard, G. E., and Heron, P. J.: The misuse of colour in science communication, *Nature*  
1207 *communications*, 11, 1-10, 2020,  
1208 <https://doi.org/10.1038/s41467-020-19160-7>

1209  
1210 Daly, M., Chorowicz, J., and Fairhead, J.: Rift basin evolution in Africa: the influence of reactivated steep basement  
1211 shear zones, *Geological Society, London, Special Publications*, 44, 309-334, 1989,  
1212 <https://doi.org/10.1144/GSL.SP.1989.044.01.17>

1213  
1214 Duclaux, G., Huismans, R. S., and May, D. A.: Rotation, narrowing, and preferential reactivation of brittle structures  
1215 during oblique rifting, *Earth and Planetary Science Letters*, 531, 115952, 2020,  
1216 <https://doi.org/10.1016/j.epsl.2019.115952>

1217  
1218 Duffy, O. B., Bell, R. E., Jackson, C. A.-L., Gawthorpe, R. L., and Whipp, P. S.: Fault growth and interactions in a  
1219 multiphase rift fault network: Horda Platform, Norwegian North Sea, *Journal of Structural Geology*, 80, 99-119,  
1220 2015,  
1221 <https://doi.org/10.1016/j.jsg.2015.08.015>

1222  
1223 Duret, T., de Borst, R., and Le Pourhiet, L.: Finite thickness of shear bands in frictional viscoplasticity and  
1224 implications for lithosphere dynamics, *Geochemistry, Geophysics, Geosystems*, 20, 5598-5616, 2019,  
1225 <https://doi.org/10.1029/2019GC008531>

1226  
1227 Ebinger, C., Yemane, T., Harding, D., Tesfaye, S., Kelley, S., and Rex, D.: Rift deflection, migration, and  
1228 propagation: Linkage of the Ethiopian and Eastern rifts, *Africa, Geological Society of America Bulletin*, 112, 163-  
1229 176, 2000,  
1230 [https://doi.org/10.1130/0016-7606\(2000\)112<163:RDMAPL>2.0.CO;2](https://doi.org/10.1130/0016-7606(2000)112<163:RDMAPL>2.0.CO;2)

1231  
1232 Gapais, D., Cobbold, P. R., Bourgeois, O., Rouby, D., and de Urreiztieta, M.: Tectonic significance of fault-slip data,  
1233 *Journal of Structural Geology*, 22, 881-888, 2000,  
1234 [https://doi.org/10.1016/S0191-8141\(00\)00015-8](https://doi.org/10.1016/S0191-8141(00)00015-8)

1235  
1236 Gassmüller, R., Lokavarapu, H., Heien, E., Puckett, E. G., and Bangerth, W.: Flexible and scalable particle-in-cell  
1237 methods with adaptive mesh refinement for geodynamic computations, *Geochemistry, Geophysics, Geosystems*,  
1238 19, 3596-3604, 2018,  
1239 <https://doi.org/10.1029/2018GC007508>

1240  
1241 Glerum, A., Brune, S., Stamps, D. S., and Strecker, M. R.: Victoria continental microplate dynamics controlled by  
1242 the lithospheric strength distribution of the East African Rift, *Nature Communications*, 11, 1-15, 2020,  
1243 <https://doi.org/10.1038/s41467-020-16176-x>

1244  
1245 Glerum, A., Thieulot, C., Fraters, M., Blom, C., and Spakman, W.: Nonlinear viscoplasticity in ASPECT:  
1246 benchmarking and applications to subduction, *Solid Earth*, 9, 267-294, 2018,

- Deleted: ., 2018.
- Formatted ... [64]
- Formatted ... [65]
- Formatted ... [66]
- Formatted ... [67]
- Formatted ... [68]
- Deleted: ., 2012.
- Formatted ... [69]
- Deleted: *Tectonophysics* 522-523, 1-33.¶
- Formatted ... [70]
- Formatted ... [71]
- Moved down [14]: Cioni, R., Franceschini, Z., Sani, F.,
- Moved down [15]: <https://doi.org/10.1038/s41467-019->
- Moved down [16]: <https://doi.org/10.1111/ter.12049¶>
- Deleted: Keir, D., 2019. Aborted propagation of th ... [73]
- Deleted: Corti, G., Philippon, M., Sani, F., Keir, D. ... [75]
- Deleted: Corti, G.,
- Deleted: ., 2007.
- Formatted ... [72]
- Formatted ... [74]
- Formatted ... [76]
- Formatted ... [77]
- Formatted ... [78]
- Deleted: *Tectonics* 26.¶
- Formatted ... [79]
- Formatted ... [80]
- Formatted ... [81]
- Moved (insertion) [16]
- Formatted ... [83]
- Field Code Changed ... [82]
- Formatted ... [84]
- Formatted ... [85]
- Moved (insertion) [14]
- Formatted ... [86]
- Moved (insertion) [15]
- Formatted ... [88]
- Field Code Changed ... [87]
- Formatted ... [89]
- Deleted: ., 2020.
- Deleted: .¶
- Formatted ... [90]
- Formatted ... [91]
- Formatted ... [92]
- Formatted ... [93]
- Formatted ... [94]
- Deleted: ., 1989.
- Formatted ... [95]
- Formatted ... [96]
- Deleted: *Geological Society, London, Special Publ* ... [97]
- Formatted ... [98]
- Formatted ... [99]
- Deleted: ., 2020.
- Formatted ... [100]
- Formatted ... [101]
- Deleted: *Earth and Planetary Science Letters* 531 ... [102]
- Formatted ... [103]
- Formatted ... [104]
- Moved (insertion) [17]
- Moved (insertion) [18]
- Formatted ... [105]
- Formatted ... [106]
- Deleted: ., 2000.
- Formatted ... [107]

1835 <https://doi.org/10.5194/se-9-267-2018>

1836 Gudmundsson, A., Simmenes, T. H., Larsen, B., and Philipp, S. L.: Effects of internal structure and local stresses

1837 on fracture propagation, deflection, and arrest in fault zones, *Journal of Structural Geology*, 32, 1643-1655, 2010,

1838 <https://doi.org/10.1016/j.jsg.2009.08.013>

1839

1840 Heidbach, O., Rajabi, M., Cui, X., Fuchs, K., Müller, B., Reinecker, J., Reiter, K., Tingay, M., Wenzel, F., and Xie,

1841 F.: The World Stress Map database release 2016: Crustal stress pattern across scales, *Tectonophysics*, 744, 484-

1842 498, 2018,

1843 <https://doi.org/10.1016/j.tecto.2018.07.007>

1844

1845 Heilman, E., Kolawole, F., Atekwana, E. A., and Mayle, M.: Controls of Basement Fabric on the Linkage of Rift

1846 Segments, *Tectonics*, 38, 1337-1366, [10.1029/2018tc005362](https://doi.org/10.1029/2018tc005362), 2019,

1847 <https://doi.org/10.1029/2018TC005362>

1848

1849 Heister, T., Dannberg, J., Gassmüller, R., and Bangerth, W.: High accuracy mantle convection simulation through

1850 modern numerical methods-II: realistic models and problems, *Geophysical Journal International*, 210, 833-851,

1851 2017,

1852 <https://doi.org/10.1029/2018TC005362>

1853

1854 Jacquey, A. B. and Cacace, M.: Multiphysics modeling of a brittle-ductile lithosphere: 2. Semi-brittle, semi-ductile

1855 deformation and damage rheology, *Journal of Geophysical Research: Solid Earth*, 125, e2019JB018475, 2020,

1856 <https://doi.org/10.1029/2019JB018475>

1857

1858 Kattenhorn, S. A., Aydin, A., and Pollard, D. D.: Joints at high angles to normal fault strike: an explanation using

1859 3-D numerical models of fault-perturbed stress fields, *Journal of structural Geology*, 22, 1-23, 2000,

1860 [https://doi.org/10.1016/S0191-8141\(99\)00130-3](https://doi.org/10.1016/S0191-8141(99)00130-3)

1861

1862 Katzman, R., ten Brink, U. S., and Lin, J.: Three-dimensional modeling of pull-apart basins: Implications for the

1863 tectonics of the Dead Sea Basin, *Journal of Geophysical Research: Solid Earth*, 100, 6295-6312, 1995,

1864 <https://doi.org/10.1029/94JB03101>

1865

1866 Keranen, K. and Klemperer, S.: Discontinuous and diachronous evolution of the Main Ethiopian Rift: Implications

1867 for development of continental rifts, *Earth and Planetary Science Letters*, 265, 96-111, 2008,

1868 <https://doi.org/10.1016/j.epsl.2007.09.038>

1869

1870 Koehn, D., Aanyu, K., Haines, S., and Sachau, T.: Rift nucleation, rift propagation and the creation of basement

1871 micro-plates within active rifts, *Tectonophysics*, 458, 105-116, 2008,

1872 <https://doi.org/10.1016/j.tecto.2007.10.003>

1873

1874 Kolawole, F., Phillips, T. B., Atekwana, E. A., and Jackson, C. A.-L.: Structural inheritance controls strain distribution

1875 during early continental rifting, rukwa rift, *Frontiers in Earth Science*, 670, 2021,

1876 <https://doi.org/10.3389/feart.2021.707869>

1877

1878 Kolawole, F., Atekwana, E. A., Laó-Dávila, D. A., Abdelsalam, M. G., Chindandali, P. R., Salima, J., and Kalindekaf,

1879 L.: Active Deformation of Malawi Rift's North Basin Hinge Zone Modulated by Reactivation of Preexisting

1880 Precambrian Shear Zone Fabric, *Tectonics*, 37, 683-704, [10.1002/2017tc004628](https://doi.org/10.1002/2017tc004628), 2018,

1881 <https://doi.org/10.1002/2017TC004628>

1882

1883 Kronbichler, M., Heister, T., and Bangerth, W.: High accuracy mantle convection simulation through modern

1884 numerical methods, *Geophysical Journal International*, 191, 12-29, 2012,

1885 <https://doi.org/10.1111/j.1365-246X.2012.05609.x>

1886

1887 Lavier, L. L., Buck, W. R., and Poliakov, A. N.: Factors controlling normal fault offset in an ideal brittle layer, *Journal*

1888 *of Geophysical Research: Solid Earth*, 105, 23431-23442, 2000,

1889 <https://doi.org/10.1029/2000JB900108>

1890

1891 Macdonald, K. C. and Fox, P.: Overlapping spreading centres: New accretion geometry on the East Pacific Rise,

1892 *Nature*, 302, 55-58, 1983,

1893 <https://doi.org/10.1038/302055a0>

1894

1895 Mills, N.: Dislocation array elements for the analysis of crack and yielded zone growth, *Journal of Materials Science*

1896 16, 1317-1331, 1981,

1897 <https://doi.org/10.1007/BF01033848>

1898

Deleted: <i>Solid Earth</i> 9, 267-294.	[130]
Formatted	[130]
Deleted: [130]	[130]
Formatted	[131]
Deleted: ., 2010.	[131]
Formatted	[132]
Deleted: <i>Journal of Structural Geology</i> 32, 1643-1655.	[132]
Formatted	[133]
Formatted	[134]
Formatted	[135]
Formatted	[136]
Deleted: ., 2018.	[137]
Formatted	[137]
Deleted: <i>Tectonophysics</i> 744, 484-498.	[138]
Formatted	[138]
Formatted	[139]
Formatted	[140]
Deleted: ., 2019.	[141]
Formatted	[141]
Deleted: <i>Tectonics</i> 38, 1337-1366.	[142]
Formatted	[142]
Formatted	[143]
Formatted	[144]
Deleted: ., 2017.	[145]
Formatted	[145]
Deleted: <i>Geophysical Journal International</i> 210, 833-851.	[146]
Formatted	[147]
Formatted	[149]
Formatted	[148]
Deleted: ., 2000.	[150]
Formatted	[150]
Deleted: <i>Journal of structural Geology</i> 22, 1-23.	[151]
Formatted	[151]
Formatted	[152]
Formatted	[153]
Formatted	[154]
Deleted: ., 1995.	[155]
Formatted	[155]
Deleted: <i>Journal of Geophysical Research: Solid Earth</i> 105, 23431-23442.	[156]
Formatted	[157]
Formatted	[158]
Formatted	[159]
Deleted: .,	[160]
Formatted	[160]
Deleted: ., 2008.	[161]
Formatted	[161]
Deleted: <i>Earth and Planetary Science Letters</i> 265, 96-111.	[162]
Formatted	[163]
Formatted	[164]
Formatted	[165]
Deleted: ., 2008.	[166]
Formatted	[166]
Formatted	[167]
Deleted: <i>Tectonophysics</i> 458, 105-116.	[168]
Formatted	[168]
Formatted	[169]
Moved (insertion) [19]	[170]
Formatted	[170]
Moved (insertion) [20]	[171]
Field Code Changed	[171]
Formatted	[172]
Formatted	[173]
Formatted	[174]



1492 Mondy, L. S., Rey, P. F., Duclaux, G., and Moresi, L.: The role of asthenospheric flow during rift propagation and  
1493 breakup, *Geology*, 46, 103-106, 2018.  
1494 <https://doi.org/10.1130/G39674.1>

1495 Morley, C.: Stress re-orientation along zones of weak fabrics in rifts: An explanation for pure extension in 'oblique'  
1496 rift segments?, *Earth and Planetary Science Letters*, 297, 667-673, 2010.  
1497 <https://doi.org/10.1016/j.epsl.2010.07.022>

1498 Morley, C.: The impact of multiple extension events, stress rotation and inherited fabrics on normal fault geometries  
1499 and evolution in the Cenozoic rift basins of Thailand, *Geological Society, London, Special Publications*, 439, 413-  
1500 445, 2017.  
1501 <https://doi.org/10.1144/SP439.3>

1502 Morley, C., Nelson, R., Patton, T., and Munn, S.: Transfer zones in the East African rift system and their relevance  
1503 to hydrocarbon exploration in rifts, *AAPG bulletin*, 74, 1234-1253, 1990.  
1504 <https://doi.org/10.1306/OC9B2475-1710-11D7-8645000102C1865D>

1505 Morley, C., Haranya, C., Phoosongsee, W., Pongwapee, S., Kornsawan, A., and Wonganan, N.: Activation of rift  
1506 oblique and rift parallel pre-existing fabrics during extension and their effect on deformation style: examples from  
1507 the rifts of Thailand, *Journal of Structural Geology*, 26, 1803-1829, 2004.  
1508 <https://doi.org/10.1016/j.jsg.2004.02.014>

1509 Morley, C. K.: Patterns of displacement along large normal faults: implications for basin evolution and fault  
1510 propagation, based on examples from East Africa, *AAPG bulletin*, 83, 613-634, 1999.  
1511 <https://doi.org/10.1306/00AA9C0A-1730-11D7-8645000102C1865D>

1512 Muhabaw, Y., Muluneh, A. A., Nugsse, K., Gebru, E. F., and Kidane, T.: Paleomagnetism of Gedemsa magmatic  
1513 segment, Main Ethiopian Rift: Implication for clockwise rotation of the segment in the Early Pleistocene,  
1514 *Tectonophysics*, 838, 229475, 2022.  
1515 <https://doi.org/10.1016/j.tecto.2022.229475>

1516 Nelson, R., Patton, T., and Morley, C.: Rift-segment interaction and its relation to hydrocarbon exploration in  
1517 continental rift systems, *AAPG bulletin*, 76, 1153-1169, 1992.  
1518 <https://doi.org/10.1306/BDF898E-1718-11D7-8645000102C1865D>

1519 Oliva, S. J., Ebinger, C. J., Rivalta, E., Williams, C. A., Wauthier, C., and Currie, C. A.: State of stress and stress  
1520 rotations: Quantifying the role of surface topography and subsurface density contrasts in magmatic rift zones  
1521 (Eastern Rift, Africa), *Earth and Planetary Science Letters*, 584, 117478, 2022.  
1522 <https://doi.org/10.1016/j.epsl.2022.117478>

1523 Philippon, M., Willingshofer, E., Sokoutis, D., Corti, G., Sani, F., Bonini, M., and Cloetingh, S.: Slip re-orientation in  
1524 oblique rifts, *Geology*, 43, 147-150, 2015.  
1525 <https://doi.org/10.1130/G36208.1>

1526 Pollard, D. D., and Aydin, A.: Propagation and linkage of oceanic ridge segments, *Journal of Geophysical Research:  
1527 Solid Earth*, 89, 10017-10028, 1984.  
1528 <https://doi.org/10.1029/JB089iB12p10017>

1529 Rose, I., Buffett, B., and Heister, T.: Stability and accuracy of free surface time integration in viscous flows, *Physics  
1530 of the Earth and Planetary Interiors*, 262, 90-100, 2017.  
1531 <https://doi.org/10.1016/j.pepi.2016.11.007>

1532 Rosendahl, B. R.: Architecture of continental rifts with special reference to East Africa, *Annual Review of Earth and  
1533 Planetary Sciences*, 15, 445, 1987.  
1534 <https://doi.org/10.1146/annurev.earth.15.050187.002305>

1535 Saria, E., Calais, E., Stamps, D., Delvaux, D., and Hartnady, C.: Present-day kinematics of the East African Rift,  
1536 *Journal of Geophysical Research: Solid Earth*, 119, 3584-3600, 2014.  
1537 <https://doi.org/10.1002/2013JB010901>

1538 Schmid, T., Schreurs, G., Warsitzka, M., and Rosenau, M.: Effect of sieving height on density and friction of brittle  
1539 analogue material: ring-shear test data of quartz sand used for analogue experiments in the Tectonic Modelling Lab  
1540 of the University of Bern, 2020a.  
1541 <https://doi.org/10.5880/fidgeo.2020.006>

- Deleted: ., 2018.
- Formatted ... [203]
- Formatted ... [204]
- Deleted: .
- Formatted ... [205]
- Formatted ... [206]
- Formatted ... [207]
- Formatted ... [208]
- Deleted: Moore Jr, J.M., Davidson, A., 1978. Rift ... [209]
- Deleted: ., 2010.
- Deleted: oblique rift segments?
- Formatted ... [210]
- Formatted ... [211]
- Formatted ... [212]
- Deleted: *Earth and Planetary Science Letters* 297 ... [213]
- Formatted ... [214]
- Formatted ... [215]
- Formatted ... [216]
- Deleted: ., 2017.
- Formatted ... [217]
- Deleted: *Geological Society, London, Special Pub...* [218]
- Formatted ... [219]
- Deleted: ., 1990.
- Formatted ... [220]
- Formatted ... [221]
- Deleted: *AAPG bulletin* 74, 1234-1253. [222]
- Formatted ... [222]
- Formatted ... [223]
- Deleted: .K., 1999.
- Formatted ... [225]
- Formatted ... [224]
- Deleted: *AAPG bulletin* 83, 613-634. [226]
- Formatted ... [226]
- Formatted ... [227]
- Formatted ... [228]
- Deleted: ., 2022.
- Formatted ... [229]
- Formatted ... [230]
- Deleted: .
- Formatted ... [231]
- Formatted ... [232]
- Formatted ... [233]
- Deleted: ., 1992.
- Formatted ... [234]
- Formatted ... [235]
- Deleted: *AAPG bulletin* 76, 1153-1169. [236]
- Formatted ... [236]
- Formatted ... [237]
- Formatted ... [238]
- Deleted: Olivia
- Deleted: ., 2022.
- Formatted ... [239]
- Formatted ... [240]
- Deleted: .)
- Formatted ... [241]
- Deleted: *Earth and Planetary Science Letters*, 58 ... [242]
- Formatted ... [243]
- Formatted ... [244]
- Formatted ... [245]
- Deleted: ., 2015.
- Formatted ... [246]
- Deleted: *Geology* 43, 147-150. [247]
- Formatted ... [247]

1676 Schmid, T., Schreurs, G., Wartsitzka, M., and Rosenau, M.: Effect of sieving height on density and friction of brittle  
1677 analogue material: Ring-shear test data of corundum sand used for analogue experiments in the Tectonic Modelling  
1678 Lab of the University of Bern (CH), 2020b.  
1679 <https://doi.org/10.5880/fidgeo.2020.005>

1680  
1681 <sup>▲</sup>Schultz-Ela, D. and Walsh, P.: Modeling of grabens extending above evaporites in Canyonlands National Park, Utah,  
1682 *Journal of Structural Geology*, 24, 247-275, 2002,  
1683 [https://doi.org/10.1016/S0191-8141\(01\)00066-9](https://doi.org/10.1016/S0191-8141(01)00066-9)

1684  
1685 <sup>▲</sup>Tingay, M., Muller, B., Reinecker, J., and Heidbach, O.: State and origin of the present-day stress field in  
1686 sedimentary basins: New results from the World Stress Map Project, Golden Rocks 2006, The 41st US Symposium  
1687 on Rock Mechanics (USRMS).

1688  
1689 Tingay, M. R., Morley, C. K., Hillis, R. R., and Meyer, J.: Present-day stress orientation in Thailand's basins, *Journal*  
1690 *of Structural Geology*, 32, 235-248, 2010.  
1691 <https://doi.org/10.1016/j.jsg.2009.11.008>

1692  
1693 Tron, V. and Brun, J.-P.: Experiments on oblique rifting in brittle-ductile systems, *Tectonophysics*, 188, 71-84,  
1694 1991,  
1695 [https://doi.org/10.1016/0040-1951\(91\)90315-1](https://doi.org/10.1016/0040-1951(91)90315-1)

1696  
1697 Trudgill, B. D.: Structural controls on drainage development in the Canyonlands grabens of southeast Utah, *AAPG*  
1698 *bulletin*, 86, 1095-1112, 2002,  
1699 <https://doi.org/10.1306/61EEDC2E-173E-11D7-8645000102C1865D>

1700  
1701 Willemse, E. J.: Segmented normal faults: Correspondence between three-dimensional mechanical models and  
1702 field data, *Journal of Geophysical Research: Solid Earth*, 102, 675-692, 1997,  
1703 <https://doi.org/10.1029/96JB01651>

1704  
1705 Willemse, E. J., Pollard, D. D., and Aydin, A.: Three-dimensional analyses of slip distributions on normal fault arrays  
1706 with consequences for fault scaling, *Journal of Structural Geology*, 18, 295-309, 1996,  
1707 [https://doi.org/10.1016/S0191-8141\(96\)80051-4](https://doi.org/10.1016/S0191-8141(96)80051-4)

1708  
1709 Withjack, M. O. and Jamison, W. R.: Deformation produced by oblique rifting, *Tectonophysics*, 126, 99-124, 1986,  
1710 [https://doi.org/10.1016/0040-1951\(86\)90222-2](https://doi.org/10.1016/0040-1951(86)90222-2)

1711  
1712 Zoback, M. J.: First- and second-order patterns of stress in the lithosphere: The World Stress Map Project, *Journal*  
1713 *of Geophysical Research: Solid Earth*, 97, 11703-11728, 1992,  
1714 <https://doi.org/10.1029/92JB00132>

1715  
1716 Zwaan, F. and Schreurs, G.: How oblique extension and structural inheritance influence rift segment interaction:  
1717 Insights from 4D analog models, *Interpretation*, 5, SD119-SD138, 2017,  
1718 <https://doi.org/10.1190/INT-2016-0063.1>

1719  
1720 Zwaan, F., Schreurs, G., Naliboff, J., and Buitter, S. J. H.: Insights into the effects of oblique extension on continental  
1721 rift interaction from 3D analogue and numerical models, *Tectonophysics*, 693, 239-260,  
1722 [10.1016/j.tecto.2016.02.036](https://doi.org/10.1016/j.tecto.2016.02.036), 2016,  
1723 <https://doi.org/10.1016/j.tecto.2016.02.036>

1724  
1725 Zwaan, F., Schreurs, G., Ritter, M., Santimano, T., and Rosenau, M.: Rheology of PDMS-corundum sand mixtures  
1726 from the Tectonic Modelling Lab of the University of Bern (CH), 2018,  
1727 <http://doi.org/10.5880/fidgeo.2018.023>

1728  
1729

Moved (insertion) [21]	
Field Code Changed	... [281]
Formatted	... [282]
Formatted	... [283]
Formatted	... [284]
Deleted: ¶	
Formatted	... [285]
Deleted: ,	
Formatted	... [286]
Deleted: , 2002.	
Formatted	... [287]
Deleted: . ¶	
Formatted	... [288]
Formatted	... [289]
Formatted	... [290]
Formatted	... [291]
Formatted	... [292]
Deleted: ,	
Formatted	... [294]
Deleted: , 1991.	
Formatted	... [295]
Deleted: . ¶	
Formatted	... [296]
Formatted	... [293]
Formatted	... [297]
Formatted	... [298]
Formatted	... [299]
Deleted: , 2002.	
Deleted: .	
Formatted	... [300]
Formatted	... [301]
Formatted	... [302]
Formatted	... [303]
Moved up [19]: B.,	
Deleted: Vetel, W., Le Gall, B., 2006. Dynamics of	... [304]
Deleted: Walsh, J.J., 2005. Geometry and growth	... [306]
Formatted	... [305]
Formatted	... [307]
Deleted: , 1997.	
Formatted	... [308]
Formatted	... [309]
Deleted: . ¶	
Formatted	... [310]
Formatted	... [311]
Formatted	... [312]
Formatted	... [313]
Formatted	... [314]
Deleted: , 1996.	
Formatted	... [315]
Deleted: <i>Journal of Structural Geology</i> 18, 295-309. ¶	
Formatted	... [316]
Formatted	... [317]
Formatted	... [318]
Formatted	... [319]
Deleted: ,	
Formatted	... [320]
Deleted: , 1986.	
Formatted	... [321]
Deleted: . ¶	
Formatted	... [322]
Formatted	... [323]
Formatted	... [324]
Formatted	... [325]

Page 39: [1] Formatted Timothy Schmid 20/02/2023 17:11:00

Font colour: Text 1

Page 39: [1] Formatted Timothy Schmid 20/02/2023 17:11:00

Font colour: Text 1

Page 39: [2] Formatted Timothy Schmid 20/02/2023 17:11:00

Font colour: Text 1

Page 39: [2] Formatted Timothy Schmid 20/02/2023 17:11:00

Font colour: Text 1

Page 39: [3] Formatted Timothy Schmid 20/02/2023 17:11:00

English (US)

Page 39: [3] Formatted Timothy Schmid 20/02/2023 17:11:00

English (US)

Page 39: [3] Formatted Timothy Schmid 20/02/2023 17:11:00

English (US)

Page 39: [4] Formatted Timothy Schmid 20/02/2023 17:11:00

Font colour: Text 1

Page 39: [5] Formatted Timothy Schmid 20/02/2023 17:11:00

Justified

Page 39: [6] Formatted Timothy Schmid 20/02/2023 17:11:00

Font colour: Text 1

Page 39: [7] Formatted Timothy Schmid 20/02/2023 17:11:00

Font colour: Text 1

Page 39: [7] Formatted Timothy Schmid 20/02/2023 17:11:00

Font colour: Text 1

Page 39: [8] Formatted Timothy Schmid 20/02/2023 17:11:00

Font colour: Text 1, English (US)

Page 39: [9] Formatted Timothy Schmid 20/02/2023 17:11:00

Font colour: Text 1, English (US)

Page 39: [10] Formatted Timothy Schmid 20/02/2023 17:11:00

Font colour: Text 1, English (US)

Page 39: [10] Formatted Timothy Schmid 20/02/2023 17:11:00

Font colour: Text 1, English (US)

Page 39: [10] Formatted Timothy Schmid 20/02/2023 17:11:00

Font colour: Text 1, English (US)

Page 39: [11] Formatted Timothy Schmid 20/02/2023 17:11:00

Font:

Page 39: [11] Formatted Timothy Schmid 20/02/2023 17:11:00

Font:

Page 39: [12] Formatted Timothy Schmid 20/02/2023 17:11:00

Font colour: Text 1

Page 39: [13] Formatted Timothy Schmid 20/02/2023 17:11:00



Font colour: Text 1

Page 39: [14] Formatted Timothy Schmid 20/02/2023 17:11:00

Font colour: Text 1

Page 39: [15] Formatted Timothy Schmid 20/02/2023 17:11:00

Font colour: Text 1

Page 39: [16] Formatted Timothy Schmid 20/02/2023 17:11:00

Font colour: Text 1

Page 39: [17] Formatted Timothy Schmid 20/02/2023 17:11:00

Font colour: Text 1

Page 39: [18] Formatted Timothy Schmid 20/02/2023 17:11:00

Font colour: Text 1

Page 39: [19] Deleted Timothy Schmid 20/02/2023 17:11:00

Page 39: [20] Formatted Timothy Schmid 20/02/2023 17:11:00

Font colour: Text 1

Page 39: [21] Formatted Timothy Schmid 20/02/2023 17:11:00

Font colour: Text 1

Page 39: [21] Formatted Timothy Schmid 20/02/2023 17:11:00

Font colour: Text 1

Page 39: [22] Formatted Timothy Schmid 20/02/2023 17:11:00

Font colour: Text 1

Page 39: [22] Formatted Timothy Schmid 20/02/2023 17:11:00

Font colour: Text 1

Page 39: [22] Formatted Timothy Schmid 20/02/2023 17:11:00

Font colour: Text 1

Page 39: [22] Formatted Timothy Schmid 20/02/2023 17:11:00

Font colour: Text 1

Page 39: [23] Formatted Timothy Schmid 20/02/2023 17:11:00

Font colour: Text 1

Page 39: [24] Moved from page 39 (Move #13) Timothy Schmid 20/02/2023 17:11:00

[Allken, V., Huismans, R.](#)

Page 39: [24] Moved from page 39 (Move #13) Timothy Schmid 20/02/2023 17:11:00

[Allken, V., Huismans, R.](#)

Page 39: [25] Formatted Timothy Schmid 20/02/2023 17:11:00

Font colour: Text 1

Page 39: [26] Formatted Timothy Schmid 20/02/2023 17:11:00

EndNote Bibliography, Justified

Page 39: [27] Change Unknown

Field Code Changed

Page 39: [28] Formatted Timothy Schmid 20/02/2023 17:11:00

Font colour: Text 1

Page 39: [29] Formatted Timothy Schmid 20/02/2023 17:11:00

Font colour: Text 1

Page 39: [30] Formatted Timothy Schmid 20/02/2023 17:11:00

Font colour: Text 1

Page 39: [31] Formatted Timothy Schmid 20/02/2023 17:11:00

Font: Not Italic, Font colour: Text 1

Page 39: [31] Formatted Timothy Schmid 20/02/2023 17:11:00

Font: Not Italic, Font colour: Text 1

Page 39: [31] Formatted Timothy Schmid 20/02/2023 17:11:00

Font: Not Italic, Font colour: Text 1

Page 39: [32] Formatted Timothy Schmid 20/02/2023 17:11:00

English (US)

Page 39: [32] Formatted Timothy Schmid 20/02/2023 17:11:00

English (US)

Page 39: [32] Formatted Timothy Schmid 20/02/2023 17:11:00

English (US)

Page 39: [33] Formatted Timothy Schmid 20/02/2023 17:11:00

Font colour: Text 1, English (US)

Page 39: [34] Formatted Timothy Schmid 20/02/2023 17:11:00

Justified

Page 39: [35] Formatted Timothy Schmid 20/02/2023 17:11:00

Font colour: Text 1, English (US)

Page 39: [35] Formatted Timothy Schmid 20/02/2023 17:11:00

Font colour: Text 1, English (US)

Page 39: [36] Formatted Timothy Schmid 20/02/2023 17:11:00

Font colour: Text 1, English (US)

Page 39: [36] Formatted Timothy Schmid 20/02/2023 17:11:00

Font colour: Text 1, English (US)

Page 39: [36] Formatted Timothy Schmid 20/02/2023 17:11:00

Font colour: Text 1, English (US)

Page 39: [37] Formatted Timothy Schmid 20/02/2023 17:11:00

Font:

Page 39: [37] Formatted Timothy Schmid 20/02/2023 17:11:00

Font:

Page 39: [38] Formatted Timothy Schmid 20/02/2023 17:11:00

Font colour: Text 1, English (US)

Page 39: [39] Formatted Timothy Schmid 20/02/2023 17:11:00

Font colour: Text 1

Page 39: [39] Formatted Timothy Schmid 20/02/2023 17:11:00

Font colour: Text 1

Page 39: [40] Formatted Timothy Schmid 20/02/2023 17:11:00

Font colour: Text 1

Page 39: [40] Formatted Timothy Schmid 20/02/2023 17:11:00

Font colour: Text 1

Page 39: [41] Formatted Timothy Schmid 20/02/2023 17:11:00

Font colour: Text 1

Page 39: [42] Formatted Timothy Schmid 20/02/2023 17:11:00

Font colour: Text 1

Page 39: [42] Formatted Timothy Schmid 20/02/2023 17:11:00

Font colour: Text 1

Page 39: [43] Deleted Timothy Schmid 20/02/2023 17:11:00

Page 39: [44] Formatted Timothy Schmid 20/02/2023 17:11:00

Font colour: Text 1

Page 39: [45] Formatted Timothy Schmid 20/02/2023 17:11:00

Justified

Page 39: [46] Formatted Timothy Schmid 20/02/2023 17:11:00

Font colour: Text 1

Page 39: [46] Formatted Timothy Schmid 20/02/2023 17:11:00

Font colour: Text 1

Page 39: [46] Formatted Timothy Schmid 20/02/2023 17:11:00

Font colour: Text 1

Page 39: [46] Formatted Timothy Schmid 20/02/2023 17:11:00

Font colour: Text 1

Page 39: [46] Formatted Timothy Schmid 20/02/2023 17:11:00

Font colour: Text 1

Page 39: [46] Formatted Timothy Schmid 20/02/2023 17:11:00

Font colour: Text 1

Page 39: [47] Deleted Timothy Schmid 20/02/2023 17:11:00

Page 39: [48] Formatted Timothy Schmid 20/02/2023 17:11:00

Font colour: Text 1

Page 39: [49] Formatted Timothy Schmid 20/02/2023 17:11:00

Justified

Page 39: [50] Formatted Timothy Schmid 20/02/2023 17:11:00

Font colour: Text 1

Page 39: [51] Formatted Timothy Schmid 20/02/2023 17:11:00

Font colour: Text 1

Page 39: [51] Formatted Timothy Schmid 20/02/2023 17:11:00

Font colour: Text 1

Page 39: [52] Formatted Timothy Schmid 20/02/2023 17:11:00

English (US)

Page 39: [53] Formatted Timothy Schmid 20/02/2023 17:11:00

Font colour: Text 1, English (US)

Page 39: [54] Formatted Timothy Schmid 20/02/2023 17:11:00

Justified

Page 39: [55] Formatted Timothy Schmid 20/02/2023 17:11:00

Font colour: Text 1

Page 39: [55] Formatted Timothy Schmid 20/02/2023 17:11:00

Font colour: Text 1

Page 39: [56] Formatted Timothy Schmid 20/02/2023 17:11:00

Font colour: Text 1

Page 39: [56] Formatted Timothy Schmid 20/02/2023 17:11:00

Font colour: Text 1

Page 39: [57] Formatted Timothy Schmid 20/02/2023 17:11:00

Font colour: Text 1

Page 39: [58] Formatted Timothy Schmid 20/02/2023 17:11:00

Font colour: Text 1

Page 39: [59] Formatted Timothy Schmid 20/02/2023 17:11:00

Justified

Page 39: [60] Formatted Timothy Schmid 20/02/2023 17:11:00

Font colour: Text 1

Page 39: [61] Formatted Timothy Schmid 20/02/2023 17:11:00

Font colour: Text 1

Page 39: [62] Formatted Timothy Schmid 20/02/2023 17:11:00

Font: Not Italic, Font colour: Text 1

Page 39: [62] Formatted Timothy Schmid 20/02/2023 17:11:00

Font: Not Italic, Font colour: Text 1

Page 39: [62] Formatted Timothy Schmid 20/02/2023 17:11:00

Font: Not Italic, Font colour: Text 1

Page 39: [63] Formatted Timothy Schmid 20/02/2023 17:11:00

Font colour: Text 1

Page 40: [64] Formatted Timothy Schmid 20/02/2023 17:11:00

Font colour: Text 1

Page 40: [64] Formatted Timothy Schmid 20/02/2023 17:11:00

Font colour: Text 1

Page 40: [64] Formatted Timothy Schmid 20/02/2023 17:11:00

Font colour: Text 1

Page 40: [65] Formatted Timothy Schmid 20/02/2023 17:11:00

Font colour: Text 1

Page 40: [65] Formatted Timothy Schmid 20/02/2023 17:11:00

Font colour: Text 1

Page 40: [66] Formatted Timothy Schmid 20/02/2023 17:11:00

English (US)

Page 40: [67] Formatted Timothy Schmid 20/02/2023 17:11:00

Font colour: Text 1

Page 40: [68] Formatted Timothy Schmid 20/02/2023 17:11:00

Justified

Page 40: [69] Formatted Timothy Schmid 20/02/2023 17:11:00

Font colour: Text 1

Page 40: [69] Formatted Timothy Schmid 20/02/2023 17:11:00

Font colour: Text 1

Page 40: [70] Formatted Timothy Schmid 20/02/2023 17:11:00

Font colour: Text 1, German (Switzerland)

Page 40: [71] Formatted Timothy Schmid 20/02/2023 17:11:00

Justified

Page 40: [72] Formatted Timothy Schmid 20/02/2023 17:11:00

Font colour: Text 1

Page 40: [73] Deleted Timothy Schmid 20/02/2023 17:11:00

Page 40: [74] Formatted Timothy Schmid 20/02/2023 17:11:00

Hyperlink, Font: Times New Roman, 12 pt, Pattern: Clear

Page 40: [75] Deleted Timothy Schmid 20/02/2023 17:11:00

Page 40: [76] Formatted Timothy Schmid 20/02/2023 17:11:00

Font colour: Text 1

Page 40: [77] Formatted Timothy Schmid 20/02/2023 17:11:00

Font colour: Text 1

Page 40: [77] Formatted Timothy Schmid 20/02/2023 17:11:00

Font colour: Text 1

Page 40: [77] Formatted Timothy Schmid 20/02/2023 17:11:00

Font colour: Text 1

Page 40: [78] Formatted Timothy Schmid 20/02/2023 17:11:00

Font colour: Text 1

Page 40: [78] Formatted Timothy Schmid 20/02/2023 17:11:00

Font colour: Text 1

Page 40: [79] Formatted Timothy Schmid 20/02/2023 17:11:00

English (US)

Page 40: [79] Formatted Timothy Schmid 20/02/2023 17:11:00

English (US)

Page 40: [79] Formatted Timothy Schmid 20/02/2023 17:11:00

English (US)

Page 40: [80] Formatted Timothy Schmid 20/02/2023 17:11:00

Default Paragraph Font, Font: Times New Roman, 12 pt, Font colour: Text 1

Page 40: [81] Formatted Timothy Schmid 20/02/2023 17:11:00

EndNote Bibliography, Justified

Page 40: [82] Change Unknown

Field Code Changed

Page 40: [83] Formatted Timothy Schmid 20/02/2023 17:11:00

English (US)

Page 40: [84] Formatted Timothy Schmid 20/02/2023 17:11:00

Font colour: Text 1

Page 40: [85] Formatted Timothy Schmid 20/02/2023 17:11:00

EndNote Bibliography, Justified

Page 40: [86] Formatted Timothy Schmid 20/02/2023 17:11:00

Font colour: Text 1

Page 40: [87] Change Unknown

Field Code Changed

Page 40: [88] Formatted Timothy Schmid 20/02/2023 17:11:00

English (US)

Page 40: [88] Formatted Timothy Schmid 20/02/2023 17:11:00

English (US)

Page 40: [88] Formatted Timothy Schmid 20/02/2023 17:11:00

English (US)

Page 40: [89] Formatted Timothy Schmid 20/02/2023 17:11:00

Normal

Page 40: [90] Formatted Timothy Schmid 20/02/2023 17:11:00

Font colour: Text 1

Page 40: [90] Formatted Timothy Schmid 20/02/2023 17:11:00

Font colour: Text 1

Page 40: [90] Formatted Timothy Schmid 20/02/2023 17:11:00

Font colour: Text 1

Page 40: [90] Formatted Timothy Schmid 20/02/2023 17:11:00

Font colour: Text 1

Page 40: [91] Formatted Timothy Schmid 20/02/2023 17:11:00

Font colour: Text 1

Page 40: [92] Formatted Timothy Schmid 20/02/2023 17:11:00

Font: Not Italic, Font colour: Text 1, French (Switzerland)

Page 40: [92] Formatted Timothy Schmid 20/02/2023 17:11:00

Font: Not Italic, Font colour: Text 1, French (Switzerland)

Page 40: [92] Formatted Timothy Schmid 20/02/2023 17:11:00

Font: Not Italic, Font colour: Text 1, French (Switzerland)

Page 40: [93] Formatted Timothy Schmid 20/02/2023 17:11:00

Font colour: Hyperlink, French (Switzerland)

Page 40: [93] Formatted Timothy Schmid 20/02/2023 17:11:00

Font colour: Hyperlink, French (Switzerland)

Page 40: [93] Formatted Timothy Schmid 20/02/2023 17:11:00

Font colour: Hyperlink, French (Switzerland)

Page 40: [94] Formatted Timothy Schmid 20/02/2023 17:11:00

Justified

Page 40: [95] Formatted Timothy Schmid 20/02/2023 17:11:00

Font colour: Text 1

Page 40: [95] Formatted Timothy Schmid 20/02/2023 17:11:00

Font colour: Text 1

Page 40: [96] Formatted Timothy Schmid 20/02/2023 17:11:00

Font colour: Text 1

Page 40: [96] Formatted Timothy Schmid 20/02/2023 17:11:00

Font colour: Text 1

Page 40: [97] Deleted Timothy Schmid 20/02/2023 17:11:00

Page 40: [98] Formatted Timothy Schmid 20/02/2023 17:11:00

Font colour: Text 1, German (Switzerland)

Page 40: [99] Formatted Timothy Schmid 20/02/2023 17:11:00

Justified

Page 40: [100] Formatted Timothy Schmid 20/02/2023 17:11:00

Font colour: Text 1

Page 40: [100] Formatted Timothy Schmid 20/02/2023 17:11:00

Font colour: Text 1

Page 40: [100] Formatted Timothy Schmid 20/02/2023 17:11:00

Font colour: Text 1

Page 40: [100] Formatted Timothy Schmid 20/02/2023 17:11:00

Font colour: Text 1

Page 40: [101] Formatted Timothy Schmid 20/02/2023 17:11:00

Font colour: Text 1

Page 40: [101] Formatted Timothy Schmid 20/02/2023 17:11:00

Font colour: Text 1

Page 40: [102] Deleted Timothy Schmid 20/02/2023 17:11:00

Page 40: [103] Formatted Timothy Schmid 20/02/2023 17:11:00

Font colour: Text 1

Page 40: [104] Formatted Timothy Schmid 20/02/2023 17:11:00

EndNote Bibliography, Justified

Page 40: [105] Formatted Timothy Schmid 20/02/2023 17:11:00

Font colour: Text 1

Page 40: [106] Formatted Timothy Schmid 20/02/2023 17:11:00

Font colour: Text 1

Page 40: [107] Formatted Timothy Schmid 20/02/2023 17:11:00

Font colour: Text 1

Page 40: [108] Formatted Timothy Schmid 20/02/2023 17:11:00

Justified

Page 40: [109] Formatted Timothy Schmid 20/02/2023 17:11:00

Font colour: Text 1

Page 40: [110] Formatted Timothy Schmid 20/02/2023 17:11:00

Font colour: Text 1

Page 40: [111] Formatted Timothy Schmid 20/02/2023 17:11:00

Font: Not Italic, Font colour: Text 1

Page 40: [111] Formatted Timothy Schmid 20/02/2023 17:11:00

Font: Not Italic, Font colour: Text 1

Page 40: [111] Formatted Timothy Schmid 20/02/2023 17:11:00

Font: Not Italic, Font colour: Text 1

Page 40: [111] Formatted Timothy Schmid 20/02/2023 17:11:00

Font: Not Italic, Font colour: Text 1

Page 40: [112] Formatted Timothy Schmid 20/02/2023 17:11:00

English (US)

Page 40: [113] Formatted Timothy Schmid 20/02/2023 17:11:00

Font colour: Text 1

Page 40: [114] Formatted Timothy Schmid 20/02/2023 17:11:00

EndNote Bibliography, Justified

Page 40: [115] Formatted Timothy Schmid 20/02/2023 17:11:00

Font colour: Text 1, English (US)

Page 40: [116] Formatted Timothy Schmid 20/02/2023 17:11:00

Justified

Page 40: [117] Formatted Timothy Schmid 20/02/2023 17:11:00

Font colour: Text 1, English (US)

Page 40: [117] Formatted Timothy Schmid 20/02/2023 17:11:00

Font colour: Text 1, English (US)

Page 40: [118] Formatted Timothy Schmid 20/02/2023 17:11:00

Font colour: Text 1, English (US)

Page 40: [118] Formatted Timothy Schmid 20/02/2023 17:11:00

Font colour: Text 1, English (US)

Page 40: [118] Formatted Timothy Schmid 20/02/2023 17:11:00

Font colour: Text 1, English (US)

Page 40: [118] Formatted Timothy Schmid 20/02/2023 17:11:00

Font colour: Text 1, English (US)

Page 40: [118] Formatted Timothy Schmid 20/02/2023 17:11:00

Font colour: Text 1, English (US)

Page 40: [118] Formatted Timothy Schmid 20/02/2023 17:11:00

Font colour: Text 1, English (US)

Page 40: [118] Formatted Timothy Schmid 20/02/2023 17:11:00

Font colour: Text 1, English (US)

Page 40: [119] Deleted Timothy Schmid 20/02/2023 17:11:00

Page 40: [120] Formatted Timothy Schmid 20/02/2023 17:11:00

English (US)

Page 40: [120] Formatted Timothy Schmid 20/02/2023 17:11:00



English (US)

Page 40: [120] Formatted Timothy Schmid 20/02/2023 17:11:00

English (US)

Page 40: [121] Formatted Timothy Schmid 20/02/2023 17:11:00

Font colour: Text 1

Page 40: [122] Formatted Timothy Schmid 20/02/2023 17:11:00

Justified

Page 40: [123] Formatted Timothy Schmid 20/02/2023 17:11:00

Font colour: Text 1, English (US)

Page 40: [123] Formatted Timothy Schmid 20/02/2023 17:11:00

Font colour: Text 1, English (US)

Page 40: [123] Formatted Timothy Schmid 20/02/2023 17:11:00

Font colour: Text 1, English (US)

Page 40: [123] Formatted Timothy Schmid 20/02/2023 17:11:00

Font colour: Text 1, English (US)

Page 40: [124] Formatted Timothy Schmid 20/02/2023 17:11:00

Font colour: Text 1, English (US)

Page 40: [124] Formatted Timothy Schmid 20/02/2023 17:11:00

Font colour: Text 1, English (US)

Page 40: [124] Formatted Timothy Schmid 20/02/2023 17:11:00

Font colour: Text 1, English (US)

Page 40: [125] Formatted Timothy Schmid 20/02/2023 17:11:00

English (US)

Page 40: [125] Formatted Timothy Schmid 20/02/2023 17:11:00

English (US)

Page 40: [125] Formatted Timothy Schmid 20/02/2023 17:11:00

English (US)

Page 40: [126] Formatted Timothy Schmid 20/02/2023 17:11:00

Font colour: Text 1

Page 40: [127] Formatted Timothy Schmid 20/02/2023 17:11:00

Justified

Page 40: [128] Formatted Timothy Schmid 20/02/2023 17:11:00

Font colour: Text 1

Page 40: [129] Formatted Timothy Schmid 20/02/2023 17:11:00

Font colour: Text 1

Page 40: [129] Formatted Timothy Schmid 20/02/2023 17:11:00

Font colour: Text 1

Page 41: [130] Formatted Timothy Schmid 20/02/2023 17:11:00

English (US)

Page 41: [130] Formatted Timothy Schmid 20/02/2023 17:11:00

English (US)

Page 41: [130] Formatted Timothy Schmid 20/02/2023 17:11:00

English (US)

Page 41: [131] Formatted Timothy Schmid 20/02/2023 17:11:00

Font colour: Text 1

Page 41: [131] Formatted Timothy Schmid 20/02/2023 17:11:00

Font colour: Text 1

Page 41: [131] Formatted Timothy Schmid 20/02/2023 17:11:00

Font colour: Text 1

Page 41: [131] Formatted Timothy Schmid 20/02/2023 17:11:00

Font colour: Text 1

Page 41: [132] Formatted Timothy Schmid 20/02/2023 17:11:00

Font colour: Text 1

Page 41: [132] Formatted Timothy Schmid 20/02/2023 17:11:00

Font colour: Text 1

Page 41: [133] Formatted Timothy Schmid 20/02/2023 17:11:00

English (US)

Page 41: [134] Formatted Timothy Schmid 20/02/2023 17:11:00

Font colour: Text 1, English (US)

Page 41: [135] Formatted Timothy Schmid 20/02/2023 17:11:00

Justified

Page 41: [136] Formatted Timothy Schmid 20/02/2023 17:11:00

Font colour: Text 1, English (US)

Page 41: [137] Formatted Timothy Schmid 20/02/2023 17:11:00

Font colour: Text 1, English (US)

Page 41: [137] Formatted Timothy Schmid 20/02/2023 17:11:00

Font colour: Text 1, English (US)

Page 41: [137] Formatted Timothy Schmid 20/02/2023 17:11:00

Font colour: Text 1, English (US)

Page 41: [138] Formatted Timothy Schmid 20/02/2023 17:11:00

Font:

Page 41: [138] Formatted Timothy Schmid 20/02/2023 17:11:00

Font:

Page 41: [139] Formatted Timothy Schmid 20/02/2023 17:11:00

Font colour: Text 1, English (US)

Page 41: [140] Formatted Timothy Schmid 20/02/2023 17:11:00

Font colour: Text 1, English (US)

Page 41: [140] Formatted Timothy Schmid 20/02/2023 17:11:00

Font colour: Text 1, English (US)

Page 41: [141] Formatted Timothy Schmid 20/02/2023 17:11:00

Font colour: Text 1, English (US)

Page 41: [141] Formatted Timothy Schmid 20/02/2023 17:11:00

Font colour: Text 1, English (US)

Page 41: [141] Formatted Timothy Schmid 20/02/2023 17:11:00

Font colour: Text 1, English (US)

Page 41: [142] Formatted Timothy Schmid 20/02/2023 17:11:00

Font colour: Auto

Page 41: [142] Formatted Timothy Schmid 20/02/2023 17:11:00

Font colour: Auto

Page 41: [143] Formatted Timothy Schmid 20/02/2023 17:11:00

Font colour: Text 1, English (US)

Page 41: [144] Formatted Timothy Schmid 20/02/2023 17:11:00

Font colour: Text 1, English (US)

Page 41: [145] Formatted Timothy Schmid 20/02/2023 17:11:00

Font colour: Text 1, English (US)

Page 41: [145] Formatted Timothy Schmid 20/02/2023 17:11:00

Font colour: Text 1, English (US)

Page 41: [145] Formatted Timothy Schmid 20/02/2023 17:11:00

Font colour: Text 1, English (US)

Page 41: [146] Deleted Timothy Schmid 20/02/2023 17:11:00

Page 41: [147] Formatted Timothy Schmid 20/02/2023 17:11:00

Font colour: Text 1, English (US)

Page 41: [148] Formatted Timothy Schmid 20/02/2023 17:11:00

Justified

Page 41: [149] Formatted Timothy Schmid 20/02/2023 17:11:00

Font colour: Text 1, English (US)

Page 41: [149] Formatted Timothy Schmid 20/02/2023 17:11:00

Font colour: Text 1, English (US)

Page 41: [149] Formatted Timothy Schmid 20/02/2023 17:11:00

Font colour: Text 1, English (US)

Page 41: [150] Formatted Timothy Schmid 20/02/2023 17:11:00

Font colour: Text 1, English (US)

Page 41: [150] Formatted Timothy Schmid 20/02/2023 17:11:00

Font colour: Text 1, English (US)

Page 41: [150] Formatted Timothy Schmid 20/02/2023 17:11:00

Font colour: Text 1, English (US)

Page 41: [151] Formatted Timothy Schmid 20/02/2023 17:11:00

English (US)

Page 41: [151] Formatted Timothy Schmid 20/02/2023 17:11:00

English (US)

Page 41: [151] Formatted Timothy Schmid 20/02/2023 17:11:00

English (US)

Page 41: [152] Formatted Timothy Schmid 20/02/2023 17:11:00

Font colour: Text 1

Page 41: [153] Formatted Timothy Schmid 20/02/2023 17:11:00

Justified

Page 41: [154] Formatted Timothy Schmid 20/02/2023 17:11:00

Font colour: Text 1, English (US)

Page 41: [154] Formatted Timothy Schmid 20/02/2023 17:11:00

Font colour: Text 1, English (US)

Page 41: [154] Formatted Timothy Schmid 20/02/2023 17:11:00

Font colour: Text 1, English (US)

Page 41: [155] Formatted Timothy Schmid 20/02/2023 17:11:00

Font colour: Text 1, English (US)

Page 41: [155] Formatted Timothy Schmid 20/02/2023 17:11:00

Font colour: Text 1, English (US)

Page 41: [155] Formatted Timothy Schmid 20/02/2023 17:11:00

Font colour: Text 1, English (US)

Page 41: [155] Formatted Timothy Schmid 20/02/2023 17:11:00

Font colour: Text 1, English (US)

Page 41: [155] Formatted Timothy Schmid 20/02/2023 17:11:00

Font colour: Text 1, English (US)

Page 41: [155] Formatted Timothy Schmid 20/02/2023 17:11:00

Font colour: Text 1, English (US)

Page 41: [155] Formatted Timothy Schmid 20/02/2023 17:11:00

Font colour: Text 1, English (US)

Page 41: [156] Deleted Timothy Schmid 20/02/2023 17:11:00

Page 41: [157] Formatted Timothy Schmid 20/02/2023 17:11:00

English (US)

Page 41: [157] Formatted Timothy Schmid 20/02/2023 17:11:00

English (US)

Page 41: [157] Formatted Timothy Schmid 20/02/2023 17:11:00

English (US)

Page 41: [158] Formatted Timothy Schmid 20/02/2023 17:11:00

Font colour: Text 1, English (US)

Page 41: [159] Formatted Timothy Schmid 20/02/2023 17:11:00

Justified

Page 41: [160] Formatted Timothy Schmid 20/02/2023 17:11:00

Font colour: Text 1, English (US)

Page 41: [161] Formatted Timothy Schmid 20/02/2023 17:11:00

Font colour: Text 1, English (US)

Page 41: [161] Formatted Timothy Schmid 20/02/2023 17:11:00

Font colour: Text 1, English (US)

Page 41: [161] Formatted Timothy Schmid 20/02/2023 17:11:00

Font colour: Text 1, English (US)

Page 41: [162] Deleted Timothy Schmid 20/02/2023 17:11:00

Page 41: [163] Formatted Timothy Schmid 20/02/2023 17:11:00

English (US)

Page 41: [164] Formatted Timothy Schmid 20/02/2023 17:11:00

Font colour: Text 1, English (US)

Page 41: [165] Formatted Timothy Schmid 20/02/2023 17:11:00

Justified

Page 41: [166] Formatted Timothy Schmid 20/02/2023 17:11:00

Font colour: Text 1, English (US)

Page 41: [167] Formatted Timothy Schmid 20/02/2023 17:11:00

Font colour: Text 1, English (US)

Page 41: [167] Formatted Timothy Schmid 20/02/2023 17:11:00

Font colour: Text 1, English (US)

Page 41: [167] Formatted Timothy Schmid 20/02/2023 17:11:00

Font colour: Text 1, English (US)

Page 41: [168] Formatted Timothy Schmid 20/02/2023 17:11:00

Font:

Page 41: [168] Formatted Timothy Schmid 20/02/2023 17:11:00

Font:

Page 41: [169] Formatted Timothy Schmid 20/02/2023 17:11:00

Font colour: Text 1, English (US)

Page 41: [170] Formatted Timothy Schmid 20/02/2023 17:11:00

Font colour: Text 1

Page 41: [170] Formatted Timothy Schmid 20/02/2023 17:11:00

Font colour: Text 1

Page 41: [171] Change Unknown

Field Code Changed

Page 41: [172] Formatted Timothy Schmid 20/02/2023 17:11:00

English (US)

Page 41: [172] Formatted Timothy Schmid 20/02/2023 17:11:00

English (US)

Page 41: [172] Formatted Timothy Schmid 20/02/2023 17:11:00

English (US)

Page 41: [173] Formatted Timothy Schmid 20/02/2023 17:11:00

Font colour: Text 1

Page 41: [174] Formatted Timothy Schmid 20/02/2023 17:11:00

Justified

Page 41: [175] Formatted Timothy Schmid 20/02/2023 17:11:00

Font colour: Text 1, English (US)

Page 41: [175] Formatted Timothy Schmid 20/02/2023 17:11:00

Font colour: Text 1, English (US)

Page 41: [175] Formatted Timothy Schmid 20/02/2023 17:11:00

Font colour: Text 1, English (US)

Page 41: [175] Formatted Timothy Schmid 20/02/2023 17:11:00

Font colour: Text 1, English (US)

Page 41: [175] Formatted Timothy Schmid 20/02/2023 17:11:00

Font colour: Text 1, English (US)

Page 41: [176] Formatted Timothy Schmid 20/02/2023 17:11:00

Font colour: Text 1, English (US)

Page 41: [176] Formatted Timothy Schmid 20/02/2023 17:11:00

Font colour: Text 1, English (US)

Page 41: [176] Formatted Timothy Schmid 20/02/2023 17:11:00

Font colour: Text 1, English (US)

Page 41: [177] Formatted Timothy Schmid 20/02/2023 17:11:00

English (US)

Page 41: [177] Formatted Timothy Schmid 20/02/2023 17:11:00

English (US)

Page 41: [177] Formatted Timothy Schmid 20/02/2023 17:11:00

English (US)

Page 41: [178] Formatted Timothy Schmid 20/02/2023 17:11:00

Font colour: Text 1

Page 41: [179] Formatted Timothy Schmid 20/02/2023 17:11:00

Justified

Page 41: [180] Formatted Timothy Schmid 20/02/2023 17:11:00

Font colour: Text 1

Page 41: [181] Formatted Timothy Schmid 20/02/2023 17:11:00

Font colour: Text 1

Page 41: [182] Deleted Timothy Schmid 20/02/2023 17:11:00

Page 41: [183] Formatted Timothy Schmid 20/02/2023 17:11:00

Font colour: Text 1

Page 41: [183] Formatted Timothy Schmid 20/02/2023 17:11:00

Font colour: Text 1

Page 41: [184] Formatted Timothy Schmid 20/02/2023 17:11:00

Font colour: Text 1

Page 41: [185] Formatted Timothy Schmid 20/02/2023 17:11:00

Font: Not Italic, Font colour: Text 1

Page 41: [185] Formatted Timothy Schmid 20/02/2023 17:11:00

Font: Not Italic, Font colour: Text 1

Page 41: [185] Formatted Timothy Schmid 20/02/2023 17:11:00

Font: Not Italic, Font colour: Text 1

Page 41: [186] Formatted Timothy Schmid 20/02/2023 17:11:00

English (US)

Page 41: [187] Formatted Timothy Schmid 20/02/2023 17:11:00

Font colour: Text 1

Page 41: [188] Formatted Timothy Schmid 20/02/2023 17:11:00

Justified

Page 41: [189] Formatted Timothy Schmid 20/02/2023 17:11:00

Font colour: Text 1

Page 41: [190] Formatted Timothy Schmid 20/02/2023 17:11:00

Justified

Page 41: [191] Formatted Timothy Schmid 20/02/2023 17:11:00

Font colour: Text 1

Page 41: [192] Formatted Timothy Schmid 20/02/2023 17:11:00

Font colour: Text 1

Page 41: [193] Formatted Timothy Schmid 20/02/2023 17:11:00

Font colour: Text 1

Page 41: [194] Formatted Timothy Schmid 20/02/2023 17:11:00

Font colour: Text 1

Page 41: [194] Formatted Timothy Schmid 20/02/2023 17:11:00

Font colour: Text 1

Page 41: [194] Formatted Timothy Schmid 20/02/2023 17:11:00

Font colour: Text 1

Page 41: [194] Formatted Timothy Schmid 20/02/2023 17:11:00

Font colour: Text 1

Page 41: [194] Formatted Timothy Schmid 20/02/2023 17:11:00

Font colour: Text 1

Page 41: [195] Formatted Timothy Schmid 20/02/2023 17:11:00

English (US)

Page 41: [195] Formatted Timothy Schmid 20/02/2023 17:11:00

English (US)

Page 41: [195] Formatted Timothy Schmid 20/02/2023 17:11:00

English (US)

Page 41: [196] Formatted Timothy Schmid 20/02/2023 17:11:00

Font colour: Text 1

Page 41: [197] Formatted Timothy Schmid 20/02/2023 17:11:00

Justified

Page 41: [198] Formatted Timothy Schmid 20/02/2023 17:11:00

Font colour: Text 1

Page 41: [199] Formatted Timothy Schmid 20/02/2023 17:11:00

Font: Not Italic, Font colour: Text 1

Page 41: [199] Formatted Timothy Schmid 20/02/2023 17:11:00

Font: Not Italic, Font colour: Text 1

Page 41: [199] Formatted Timothy Schmid 20/02/2023 17:11:00

Font: Not Italic, Font colour: Text 1

Page 41: [200] Formatted Timothy Schmid 20/02/2023 17:11:00

English (US)

Page 41: [200] Formatted Timothy Schmid 20/02/2023 17:11:00

English (US)

Page 41: [200] Formatted Timothy Schmid 20/02/2023 17:11:00

English (US)

Page 41: [201] Formatted Timothy Schmid 20/02/2023 17:11:00

Font colour: Text 1

Page 41: [202] Formatted Timothy Schmid 20/02/2023 17:11:00

Justified

Page 42: [203] Formatted Timothy Schmid 20/02/2023 17:11:00

Font colour: Text 1

Page 42: [203] Formatted Timothy Schmid 20/02/2023 17:11:00

Font colour: Text 1

Page 42: [203] Formatted Timothy Schmid 20/02/2023 17:11:00

Font colour: Text 1

Page 42: [204] Formatted Timothy Schmid 20/02/2023 17:11:00

Font colour: Text 1

Page 42: [205] Formatted Timothy Schmid 20/02/2023 17:11:00

Font: Not Italic, Font colour: Text 1

Page 42: [205] Formatted Timothy Schmid 20/02/2023 17:11:00

Font: Not Italic, Font colour: Text 1

Page 42: [205] Formatted Timothy Schmid 20/02/2023 17:11:00

Font: Not Italic, Font colour: Text 1

Page 42: [206] Formatted Timothy Schmid 20/02/2023 17:11:00

English (US)

Page 42: [206] Formatted Timothy Schmid 20/02/2023 17:11:00

English (US)

Page 42: [206] Formatted Timothy Schmid 20/02/2023 17:11:00

English (US)

Page 42: [207] Formatted Timothy Schmid 20/02/2023 17:11:00

Font colour: Text 1

Page 42: [208] Formatted Timothy Schmid 20/02/2023 17:11:00

EndNote Bibliography, Justified

Page 42: [209] Deleted Timothy Schmid 20/02/2023 17:11:00

Page 42: [210] Formatted Timothy Schmid 20/02/2023 17:11:00

Font colour: Text 1

Page 42: [211] Formatted Timothy Schmid 20/02/2023 17:11:00

Font colour: Text 1



Page 42: [212] Formatted Timothy Schmid 20/02/2023 17:11:00

Font colour: Text 1

Page 42: [213] Deleted Timothy Schmid 20/02/2023 17:11:00

Page 42: [214] Formatted Timothy Schmid 20/02/2023 17:11:00

English (US)

Page 42: [215] Formatted Timothy Schmid 20/02/2023 17:11:00

Font colour: Text 1

Page 42: [216] Formatted Timothy Schmid 20/02/2023 17:11:00

Justified

Page 42: [217] Formatted Timothy Schmid 20/02/2023 17:11:00

Font colour: Text 1

Page 42: [217] Formatted Timothy Schmid 20/02/2023 17:11:00

Font colour: Text 1

Page 42: [218] Deleted Timothy Schmid 20/02/2023 17:11:00

Page 42: [219] Formatted Timothy Schmid 20/02/2023 17:11:00

Font colour: Text 1

Page 42: [220] Formatted Timothy Schmid 20/02/2023 17:11:00

Font colour: Text 1

Page 42: [221] Formatted Timothy Schmid 20/02/2023 17:11:00

Font colour: Text 1

Page 42: [221] Formatted Timothy Schmid 20/02/2023 17:11:00

Font colour: Text 1

Page 42: [222] Formatted Timothy Schmid 20/02/2023 17:11:00

Font:

Page 42: [222] Formatted Timothy Schmid 20/02/2023 17:11:00

Font:

Page 42: [223] Formatted Timothy Schmid 20/02/2023 17:11:00

EndNote Bibliography, Justified

Page 42: [224] Formatted Timothy Schmid 20/02/2023 17:11:00

Justified

Page 42: [225] Formatted Timothy Schmid 20/02/2023 17:11:00

Font colour: Text 1

Page 42: [225] Formatted Timothy Schmid 20/02/2023 17:11:00

Font colour: Text 1

Page 42: [226] Formatted Timothy Schmid 20/02/2023 17:11:00

English (US)

Page 42: [227] Formatted Timothy Schmid 20/02/2023 17:11:00

Font colour: Text 1

Page 42: [228] Formatted Timothy Schmid 20/02/2023 17:11:00

EndNote Bibliography, Justified

Page 42: [229] Formatted Timothy Schmid 20/02/2023 17:11:00

Font colour: Text 1

Page 42: [229] Formatted Timothy Schmid 20/02/2023 17:11:00

Font colour: Text 1

Page 42: [229] Formatted Timothy Schmid 20/02/2023 17:11:00

Font colour: Text 1

Page 42: [230] Formatted Timothy Schmid 20/02/2023 17:11:00

Font colour: Text 1

Page 42: [231] Formatted Timothy Schmid 20/02/2023 17:11:00

Font colour: Text 1

Page 42: [231] Formatted Timothy Schmid 20/02/2023 17:11:00

Font colour: Text 1

Page 42: [231] Formatted Timothy Schmid 20/02/2023 17:11:00

Font colour: Text 1

Page 42: [231] Formatted Timothy Schmid 20/02/2023 17:11:00

Font colour: Text 1

Page 42: [232] Formatted Timothy Schmid 20/02/2023 17:11:00

Font colour: Text 1

Page 42: [233] Formatted Timothy Schmid 20/02/2023 17:11:00

EndNote Bibliography, Justified

Page 42: [234] Formatted Timothy Schmid 20/02/2023 17:11:00

Font colour: Text 1

Page 42: [235] Formatted Timothy Schmid 20/02/2023 17:11:00

Font colour: Text 1

Page 42: [235] Formatted Timothy Schmid 20/02/2023 17:11:00

Font colour: Text 1

Page 42: [236] Formatted Timothy Schmid 20/02/2023 17:11:00

English (US)

Page 42: [237] Formatted Timothy Schmid 20/02/2023 17:11:00

Font colour: Text 1

Page 42: [238] Formatted Timothy Schmid 20/02/2023 17:11:00

Justified

Page 42: [239] Formatted Timothy Schmid 20/02/2023 17:11:00

Font colour: Text 1

Page 42: [239] Formatted Timothy Schmid 20/02/2023 17:11:00

Font colour: Text 1

Page 42: [240] Formatted Timothy Schmid 20/02/2023 17:11:00

Font colour: Text 1

Page 42: [241] Formatted Timothy Schmid 20/02/2023 17:11:00

Font colour: Text 1

Page 42: [242] Deleted Timothy Schmid 20/02/2023 17:11:00

Page 42: [243] Formatted Timothy Schmid 20/02/2023 17:11:00

Font colour: Text 1

Page 42: [244] Formatted Timothy Schmid 20/02/2023 17:11:00

Justified

Page 42: [245] Formatted Timothy Schmid 20/02/2023 17:11:00

Font colour: Text 1

Page 42: [246] Formatted Timothy Schmid 20/02/2023 17:11:00

Font colour: Text 1

Page 42: [246] Formatted Timothy Schmid 20/02/2023 17:11:00

Font colour: Text 1

Page 42: [247] Formatted Timothy Schmid 20/02/2023 17:11:00

Font:

Page 42: [247] Formatted Timothy Schmid 20/02/2023 17:11:00

Font:

Page 42: [248] Formatted Timothy Schmid 20/02/2023 17:11:00

Font colour: Text 1

Page 42: [249] Formatted Timothy Schmid 20/02/2023 17:11:00

EndNote Bibliography, Justified

Page 42: [250] Formatted Timothy Schmid 20/02/2023 17:11:00

Font colour: Text 1

Page 42: [251] Formatted Timothy Schmid 20/02/2023 17:11:00

Font colour: Text 1

Page 42: [251] Formatted Timothy Schmid 20/02/2023 17:11:00

Font colour: Text 1

Page 42: [252] Deleted Timothy Schmid 20/02/2023 17:11:00

Page 42: [253] Formatted Timothy Schmid 20/02/2023 17:11:00

English (US)

Page 42: [253] Formatted Timothy Schmid 20/02/2023 17:11:00

English (US)

Page 42: [253] Formatted Timothy Schmid 20/02/2023 17:11:00

English (US)

Page 42: [254] Formatted Timothy Schmid 20/02/2023 17:11:00

Font colour: Text 1

Page 42: [255] Formatted Timothy Schmid 20/02/2023 17:11:00

Justified

Page 42: [256] Formatted Timothy Schmid 20/02/2023 17:11:00

Font colour: Text 1

Page 42: [257] Formatted Timothy Schmid 20/02/2023 17:11:00

Font colour: Text 1

Page 42: [257] Formatted Timothy Schmid 20/02/2023 17:11:00

Font colour: Text 1

Page 42: [258] Deleted Timothy Schmid 20/02/2023 17:11:00

Page 42: [259] Formatted Timothy Schmid 20/02/2023 17:11:00

Font:

Page 42: [259] Formatted Timothy Schmid 20/02/2023 17:11:00

Font:

Page 42: [260] Formatted Timothy Schmid 20/02/2023 17:11:00

Font colour: Text 1, English (US)

Page 42: [261] Formatted Timothy Schmid 20/02/2023 17:11:00

Font colour: Text 1

Page 42: [261] Formatted Timothy Schmid 20/02/2023 17:11:00

Font colour: Text 1

Page 42: [262] Formatted Timothy Schmid 20/02/2023 17:11:00

Font colour: Text 1

Page 42: [262] Formatted Timothy Schmid 20/02/2023 17:11:00

Font colour: Text 1

Page 42: [263] Deleted Timothy Schmid 20/02/2023 17:11:00

Page 42: [264] Formatted Timothy Schmid 20/02/2023 17:11:00

English (US)

Page 42: [264] Formatted Timothy Schmid 20/02/2023 17:11:00

English (US)

Page 42: [264] Formatted Timothy Schmid 20/02/2023 17:11:00

English (US)

Page 42: [265] Formatted Timothy Schmid 20/02/2023 17:11:00

Font colour: Text 1

Page 42: [266] Formatted Timothy Schmid 20/02/2023 17:11:00

Justified

Page 42: [267] Formatted Timothy Schmid 20/02/2023 17:11:00

Font colour: Text 1

Page 42: [268] Formatted Timothy Schmid 20/02/2023 17:11:00

Font colour: Text 1

Page 42: [268] Formatted Timothy Schmid 20/02/2023 17:11:00

Font colour: Text 1

Page 42: [268] Formatted Timothy Schmid 20/02/2023 17:11:00

Font colour: Text 1

Page 42: [269] Formatted Timothy Schmid 20/02/2023 17:11:00

Font colour: Text 1

Page 42: [269] Formatted Timothy Schmid 20/02/2023 17:11:00

Font colour: Text 1

Page 42: [269] Formatted Timothy Schmid 20/02/2023 17:11:00

Font colour: Text 1

Page 42: [269] Formatted Timothy Schmid 20/02/2023 17:11:00

Font colour: Text 1

Page 42: [270] Formatted Timothy Schmid 20/02/2023 17:11:00

EndNote Bibliography

Page 42: [271] Formatted Timothy Schmid 20/02/2023 17:11:00

Font colour: Auto

Page 42: [271] Formatted Timothy Schmid 20/02/2023 17:11:00

Font colour: Auto

Page 42: [272] Formatted Timothy Schmid 20/02/2023 17:11:00

Font colour: Text 1, English (US)

Page 42: [273] Formatted Timothy Schmid 20/02/2023 17:11:00

Justified

Page 42: [274] Formatted Timothy Schmid 20/02/2023 17:11:00

Font colour: Text 1

Page 42: [275] Deleted Timothy Schmid 20/02/2023 17:11:00

Page 42: [276] Formatted Timothy Schmid 20/02/2023 17:11:00

Font colour: Text 1

Page 42: [277] Deleted Timothy Schmid 20/02/2023 17:11:00

Page 42: [278] Formatted Timothy Schmid 20/02/2023 17:11:00

Font colour: Text 1, English (US)

Page 42: [278] Formatted Timothy Schmid 20/02/2023 17:11:00

Font colour: Text 1, English (US)

Page 42: [279] Formatted Timothy Schmid 20/02/2023 17:11:00

Font colour: Text 1

Page 42: [280] Formatted Timothy Schmid 20/02/2023 17:11:00

English (US)

Page 42: [280] Formatted Timothy Schmid 20/02/2023 17:11:00

English (US)

Page 43: [281] Change Unknown

Field Code Changed

Page 43: [282] Formatted Timothy Schmid 20/02/2023 17:11:00

English (US)

Page 43: [282] Formatted Timothy Schmid 20/02/2023 17:11:00

English (US)

Page 43: [283] Formatted Timothy Schmid 20/02/2023 17:11:00

Font colour: Text 1

Page 43: [284] Formatted Timothy Schmid 20/02/2023 17:11:00

Justified

Page 43: [285] Formatted Timothy Schmid 20/02/2023 17:11:00

Font colour: Text 1

Page 43: [286] Formatted Timothy Schmid 20/02/2023 17:11:00

Font colour: Text 1

Page 43: [287] Formatted Timothy Schmid 20/02/2023 17:11:00

Font colour: Text 1

Page 43: [288] Formatted Timothy Schmid 20/02/2023 17:11:00

Font: Not Italic, Font colour: Text 1

Page 43: [288] Formatted Timothy Schmid 20/02/2023 17:11:00

Font: Not Italic, Font colour: Text 1

Page 43: [288] Formatted Timothy Schmid 20/02/2023 17:11:00

Font: Not Italic, Font colour: Text 1

Page 43: [289] Formatted Timothy Schmid 20/02/2023 17:11:00

English (US)

Page 43: [289] Formatted Timothy Schmid 20/02/2023 17:11:00

English (US)

Page 43: [289] Formatted Timothy Schmid 20/02/2023 17:11:00

English (US)

Page 43: [290] Formatted Timothy Schmid 20/02/2023 17:11:00

Font colour: Text 1

Page 43: [291] Formatted Timothy Schmid 20/02/2023 17:11:00

Justified

Page 43: [292] Formatted Timothy Schmid 20/02/2023 17:11:00

Font colour: Text 1

Page 43: [293] Formatted Timothy Schmid 20/02/2023 17:11:00

Justified

Page 43: [294] Formatted Timothy Schmid 20/02/2023 17:11:00

Font colour: Text 1

Page 43: [295] Formatted Timothy Schmid 20/02/2023 17:11:00

Font colour: Text 1

Page 43: [296] Formatted Timothy Schmid 20/02/2023 17:11:00

Font: Not Italic, Font colour: Text 1

Page 43: [296] Formatted Timothy Schmid 20/02/2023 17:11:00

Font: Not Italic, Font colour: Text 1

Page 43: [296] Formatted Timothy Schmid 20/02/2023 17:11:00

Font: Not Italic, Font colour: Text 1

Page 43: [297] Formatted Timothy Schmid 20/02/2023 17:11:00

English (US)

Page 43: [297] Formatted Timothy Schmid 20/02/2023 17:11:00

English (US)

Page 43: [297] Formatted Timothy Schmid 20/02/2023 17:11:00

English (US)

Page 43: [298] Formatted Timothy Schmid 20/02/2023 17:11:00

Font colour: Text 1

Page 43: [299] Formatted Timothy Schmid 20/02/2023 17:11:00

Justified

Page 43: [300] Formatted Timothy Schmid 20/02/2023 17:11:00

Font colour: Text 1

Page 43: [301] Formatted Timothy Schmid 20/02/2023 17:11:00

Font colour: Text 1

Page 43: [302] Formatted Timothy Schmid 20/02/2023 17:11:00

Font colour: Text 1

Page 43: [302] Formatted Timothy Schmid 20/02/2023 17:11:00

Font colour: Text 1

Page 43: [302] Formatted Timothy Schmid 20/02/2023 17:11:00

Font colour: Text 1

Page 43: [302] Formatted Timothy Schmid 20/02/2023 17:11:00

Font colour: Text 1

Page 43: [303] Formatted Timothy Schmid 20/02/2023 17:11:00

English (US)

Page 43: [303] Formatted Timothy Schmid 20/02/2023 17:11:00

English (US)

Page 43: [303] Formatted Timothy Schmid 20/02/2023 17:11:00

English (US)

Page 43: [304] Deleted Timothy Schmid 20/02/2023 17:11:00

Page 43: [305] Formatted Timothy Schmid 20/02/2023 17:11:00

Font colour: Text 1

Page 43: [306] Deleted Timothy Schmid 20/02/2023 17:11:00

Page 43: [307] Formatted Timothy Schmid 20/02/2023 17:11:00

Font colour: Text 1

Page 43: [308] Formatted Timothy Schmid 20/02/2023 17:11:00

Font colour: Text 1

Page 43: [309] Formatted Timothy Schmid 20/02/2023 17:11:00

Font colour: Text 1

Page 43: [309] Formatted Timothy Schmid 20/02/2023 17:11:00

Font colour: Text 1

Page 43: [309] Formatted Timothy Schmid 20/02/2023 17:11:00

Font colour: Text 1

Page 43: [310] Formatted Timothy Schmid 20/02/2023 17:11:00

Font: Not Italic, Font colour: Text 1

Page 43: [310] Formatted Timothy Schmid 20/02/2023 17:11:00

Font: Not Italic, Font colour: Text 1

Page 43: [310] Formatted Timothy Schmid 20/02/2023 17:11:00

Font: Not Italic, Font colour: Text 1

Page 43: [311] Formatted Timothy Schmid 20/02/2023 17:11:00

English (US)

Page 43: [311] Formatted Timothy Schmid 20/02/2023 17:11:00

English (US)

Page 43: [311] Formatted Timothy Schmid 20/02/2023 17:11:00

English (US)

Page 43: [312] Formatted Timothy Schmid 20/02/2023 17:11:00

Font colour: Text 1

Page 43: [313] Formatted Timothy Schmid 20/02/2023 17:11:00

Justified

Page 43: [314] Formatted Timothy Schmid 20/02/2023 17:11:00

Font colour: Text 1

Page 43: [314] Formatted Timothy Schmid 20/02/2023 17:11:00

Font colour: Text 1

Page 43: [314] Formatted Timothy Schmid 20/02/2023 17:11:00

Font colour: Text 1

Page 43: [315] Formatted Timothy Schmid 20/02/2023 17:11:00

Font colour: Text 1

Page 43: [315] Formatted Timothy Schmid 20/02/2023 17:11:00

Font colour: Text 1

Page 43: [316] Formatted Timothy Schmid 20/02/2023 17:11:00

English (US)

Page 43: [316] Formatted Timothy Schmid 20/02/2023 17:11:00

English (US)

Page 43: [316] Formatted Timothy Schmid 20/02/2023 17:11:00

English (US)

Page 43: [317] Formatted Timothy Schmid 20/02/2023 17:11:00

Font colour: Text 1

Page 43: [318] Formatted Timothy Schmid 20/02/2023 17:11:00

Justified

Page 43: [319] Formatted Timothy Schmid 20/02/2023 17:11:00

Font colour: Text 1

Page 43: [320] Formatted Timothy Schmid 20/02/2023 17:11:00

Font colour: Text 1

Page 43: [320] Formatted Timothy Schmid 20/02/2023 17:11:00

Font colour: Text 1

Page 43: [321] Formatted Timothy Schmid 20/02/2023 17:11:00

Font colour: Text 1

Page 43: [322] Formatted Timothy Schmid 20/02/2023 17:11:00

Font: Not Italic, Font colour: Text 1

Page 43: [322] Formatted Timothy Schmid 20/02/2023 17:11:00

Font: Not Italic, Font colour: Text 1



Page 43: [322] Formatted Timothy Schmid 20/02/2023 17:11:00

Font: Not Italic, Font colour: Text 1

Page 43: [323] Formatted Timothy Schmid 20/02/2023 17:11:00

English (US)

Page 43: [323] Formatted Timothy Schmid 20/02/2023 17:11:00

English (US)

Page 43: [323] Formatted Timothy Schmid 20/02/2023 17:11:00

English (US)

Page 43: [324] Formatted Timothy Schmid 20/02/2023 17:11:00

Font colour: Text 1

Page 43: [325] Formatted Timothy Schmid 20/02/2023 17:11:00

Justified

Page 43: [326] Formatted Timothy Schmid 20/02/2023 17:11:00

Font colour: Text 1

Page 43: [327] Formatted Timothy Schmid 20/02/2023 17:11:00

Font colour: Text 1

Page 43: [327] Formatted Timothy Schmid 20/02/2023 17:11:00

Font colour: Text 1

Page 43: [327] Formatted Timothy Schmid 20/02/2023 17:11:00

Font colour: Text 1

Page 43: [327] Formatted Timothy Schmid 20/02/2023 17:11:00

Font colour: Text 1

Page 43: [327] Formatted Timothy Schmid 20/02/2023 17:11:00

Font colour: Text 1

Page 43: [328] Formatted Timothy Schmid 20/02/2023 17:11:00

Font colour: Text 1

Page 43: [328] Formatted Timothy Schmid 20/02/2023 17:11:00

Font colour: Text 1

Page 43: [328] Formatted Timothy Schmid 20/02/2023 17:11:00

Font colour: Text 1

Page 43: [328] Formatted Timothy Schmid 20/02/2023 17:11:00

Font colour: Text 1

Page 43: [329] Formatted Timothy Schmid 20/02/2023 17:11:00

English (US)

Page 43: [329] Formatted Timothy Schmid 20/02/2023 17:11:00

English (US)

Page 43: [329] Formatted Timothy Schmid 20/02/2023 17:11:00

English (US)

Page 43: [330] Formatted Timothy Schmid 20/02/2023 17:11:00

Font colour: Text 1

Page 43: [331] Formatted Timothy Schmid 20/02/2023 17:11:00

Justified

Page 43: [332] Formatted Timothy Schmid 20/02/2023 17:11:00

Font colour: Text 1

Page 43: [333] Formatted Timothy Schmid 20/02/2023 17:11:00

Font colour: Text 1

Page 43: [333] Formatted Timothy Schmid 20/02/2023 17:11:00

Font colour: Text 1

Page 43: [334] Formatted Timothy Schmid 20/02/2023 17:11:00

Default Paragraph Font, Font: Times New Roman, 12 pt, Font colour: Text 1, Border: : (No border)

Page 43: [335] Formatted Timothy Schmid 20/02/2023 17:11:00

Font colour: Text 1

Page 43: [336] Formatted Timothy Schmid 20/02/2023 17:11:00

Font colour: Text 1, English (US)

Page 43: [336] Formatted Timothy Schmid 20/02/2023 17:11:00

Font colour: Text 1, English (US)

Page 43: [336] Formatted Timothy Schmid 20/02/2023 17:11:00

Font colour: Text 1, English (US)

Page 43: [336] Formatted Timothy Schmid 20/02/2023 17:11:00

Font colour: Text 1, English (US)

Page 43: [337] Formatted Timothy Schmid 20/02/2023 17:11:00

Font colour: Text 1, English (US)

Page 43: [337] Formatted Timothy Schmid 20/02/2023 17:11:00

Font colour: Text 1, English (US)

Page 43: [337] Formatted Timothy Schmid 20/02/2023 17:11:00

Font colour: Text 1, English (US)

Page 43: [338] Formatted Timothy Schmid 20/02/2023 17:11:00

English (US)

Page 43: [338] Formatted Timothy Schmid 20/02/2023 17:11:00

English (US)

Page 43: [338] Formatted Timothy Schmid 20/02/2023 17:11:00

English (US)

Page 43: [339] Formatted Timothy Schmid 20/02/2023 17:11:00

Font colour: Text 1

Page 43: [340] Formatted Timothy Schmid 20/02/2023 17:11:00

Justified

Page 43: [341] Formatted Timothy Schmid 20/02/2023 17:11:00

Font colour: Text 1

Page 43: [342] Formatted Timothy Schmid 20/02/2023 17:11:00

Font colour: Text 1

Page 43: [343] Formatted Timothy Schmid 20/02/2023 17:11:00

Font colour: Text 1